E.O. Paton Electric Welding Institute of the National Academy of Sciences of Ukraine

International Scientific-Technical and Production Journal

The Paton WELDING JOURNAL

December **2017**
No. 12

Published since 2000

English translation of the monthly «Avtomaticheskaya Svarka» (Automatic Welding) journal published in Russian since 1948

EDITORIAL BOARD
Editor-in-Chief
B.E. Paton

Scientists of PWI, Kiev
S.I. Kuchuk-Yatsenko (*vice-chief ed.***),**
V.N. Lipodaev (*vice-chief ed.***),**
Yu.S. Borisov, G.M. Grigorenko,
A.T. Zelnichenko, V.V. Knysh,
I.V. Krivtsun, Yu.N. Lankin,
L.M. Lobanov, V.D. Poznyakov,
I.A. Ryabtsev, K.A. Yushchenko

Scientists of Ukrainian Universities
V.V. Dmitrik, NTU «KhPI», Kharkov
V.V. Kvasnitsky, NTUU «KPI», Kiev
V.D. Kuznetsov, NTUU «KPI», Kiev

Foreign Scientists
N.P. Alyoshin
N.E. Bauman MSTU, Moscow, Russia
Guan Qiao
Beijing Aeronautical Institute, China
A.S. Zubchenko
DB «Gidropress», Podolsk, Russia
M. Zinigrad
Ariel University, Israel
V.I. Lysak
Volgograd STU, Russia
Ya. Pilarczyk
Welding Institute, Gliwice, Poland
U. Reisgen
Welding and Joining Institute, Aachen, Germany
G.A. Turichin
St. Petersburg SPU, Russia

Founders
E.O. Paton Electric Welding Institute, NASU
International Association «Welding»

Publisher
International Association «Welding»

Translators
A.A. Fomin, O.S. Kurochko, I.N. Kutianova
Editor
N.G. Khomenko
Electron galley
D.I. Sereda, T.Yu. Snegiryova

Address
E.O. Paton Electric Welding Institute,
International Association «Welding»
11 Kazimir Malevich Str. (former Bozhenko Str.),
03150, Kiev, Ukraine
Tel.: (38044) 200 60 16, 200 82 77
Fax: (38044) 200 82 77, 200 81 45
E-mail: journal@paton.kiev.ua
www.patonpublishinghouse.com

State Registration Certificate
KV 4790 of 09.01.2001
ISSN 0957-798X
doi.org/10.15407/tpwj

Subscriptions
$348, 12 issues per year,
air postage and packaging included.
Back issues available.

All rights reserved.
This publication and each of the articles contained herein are protected by copyright.
Permission to reproduce material contained in this journal must be obtained in writing from the Publisher.

CONTENTS

© PWI, International Association «Welding», 2017

XVI INTERNATIONAL INDUSTRIAL FORUM

On November 21–24, 2017, the XVI International Forum was held in Kiev at the International Exhibition Center. Starting from 2005, the Forum has been included into the list of leading world industrial exhibitions, officially certified and recognized by UFI — the Global Association of the Exhibition Industry. Every year it confirms its status of the most significant event in Ukraine on machine-building topics.

Some statistics:

- 337 enterprises took part in the event;
- 29 world countries presented their technologies and equipment;
- Total exposition space was 17000 m^2;
- 10500 specialists attended the Forum.

International Industrial Forum included specialized industrial exhibitions in the field of metalworking, machine-building and related industries, as well as an extensive program of research and practical conferences, seminars and presentations of Forum participants.

The list of exhibitions included:

- METALWORKING (metalworking technologies, equipment);
- UKRUSEDTECH (brokerage appliances, equipment);
- UKRFOUNDRY (foundry equipment and technologies);
- UKRWELDING (technologies, equipment and materials);
- HYDRAULICS. PNEUMATICS;
- BEARINGS (rolling, sliding bearings, loose parts: balls, rollers, clamping sleeves, technologies, equipment and tools for bearings manufacture);
- UKRPROMAUTOMATION (industrial automation, CAM systems, automation of industrial facilities);
- HOISTING AND TRANSPORTATION, STOREHOUSE EQUIPMENT;
- SPECIMENS, STANDARDS, TEMPLATES, INSTRUMENTS (controlling and measuring instruments, laboratory and testing equipment, metrology, certification);
- INDUSTRIAL SAFETY (protection means, working area safety).

Leading industrial enterprises of Ukraine, as well as companies from the CIS and foreign countries participated in the exhibition.

In UKRWELDING exposition about 60 companies demonstrated their products, including those from Turkey (2), China (2), Czech Republic (1), Belarus (1), Ireland (1) and Ukraine (53). The following Ukrainian companies took part in the exhibition: Aramis, Vistec, Vitapolis, Donmet, Tekhmash, Zont, Idel, Navko-Tekh, Sumy-Electrode, Fronius Ukraine, Binzel Ukraine and many others.

The booth of the E.O. Paton Electric Welding Institute Publishing House attracted a lot of interest of exhibition visitors and participants. It displayed «The Paton Welding Journal», «Technical Diagnostics and Nondestructive Testing», «Sovremennaya Elektrometallurgiya» journals, as well as books, conference proceedings and thematic collections on welding and related technologies.

In addition to functioning of the main Forum expositions, scientific-technical conferences, seminars and presentations were conducted for three days. Scientific-practical conference «Present-Day Problems of Welding Industry», organized by Welders' Society of Ukraine and the conference, organized by the Ukrainian Society for Non-Destructive Testing and Technical Diagnostics, aroused particular interest.

Summing up we should note active attendance of the exhibition, great diversity in the design of the

Address by S.I. Kubiv, First Vice Prime Minister of Ukraine at China-Ukraine Science, Technology and Innovation Exhibition

Opening ceremony of «Innovation Forum»

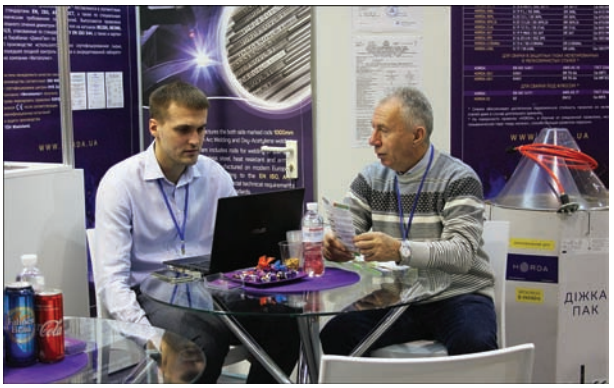

At Vitapolis booth

At Binzel Ukraine booth

At Fronius Ukraine booth

booths and their information content. In the opinion of exhibition participants and visitors, the Forum in 2017 exceeded all expectations: clearly there is progress in the field of innovative proposals from exhibitors and increased interest of visitors to the exposition.

II International Forum «Innovation Market» — technologies of the future today under the motto of «Science-Business-Power» was held in parallel with the Industrial Forum on the same days. This is already the second meeting of innovators, local and foreign investors and businessmen, representatives of the authorities for combining their efforts in development of innovation market in Ukraine. The Forum was held under the patronage of the Cabinet of Ministers of Ukraine and with the support of the Ministry of Economic Development and Trade, the Ministry of Education and Science, the National Academy of Sciences of Ukraine, and CSTEC — the Chinese Center for the Exchange of Scientific and Technological Information. The International Exhibition Center was the chief administrator.

The objective of the Forum is demonstration of the best innovations in all the spheres of economy of Ukraine, and attracting investments for their introduction. The Forum brought together almost 220 exhibitors — universities, research institutes, manufacturing companies, Start-up projects of Ukraine, as well as leading research institutions and manufacturing companies of China. Speakers and experts participating in the event included such well-known names as Ch. Whitehead (USA), Prof. of Business Law, and Director of «Law, Technology and Entrepreneurship» Program of Cornell University, G. Olsen (USA) — scientist and entrepreneur, world's third space tourist, T. Catran — developer of Startup ecosystems, and other experts known in their fields. Heads of Ukrainian government, leading ministries and specialized committees of the Verkhovna Rada of Ukraine also participated in the Forum activities.

It should be specially mentioned that China-Ukraine Science, Technology and Innovation Exhibition was held within the Forum. More than 90 leading institutions and manufacturing companies of China participated in it, including E.O. Paton Chinese-Ukrainian Institute of Welding. Ukrainian-Chinese Round Table for young entrepreneurs was also held, as well as Forum of Ukrainian-Chinese cooperation.

By materials of IEC Press-service

doi.org/10.15407/tpwj2017.12.01

AUTOMATED DESIGNING OF MANUFACTURABLE HIGH-TEMPERATURE ALLOY COMPOSITION ON NICKEL BASE FOR MANUFACTURE OF ALL-CAST NOZZLE APPARATUSES

S.V. GAJDUK[1], **V.V. KONONOV**[1] and **V.V. KURENKOVA**[2]
[1]Zaporozhye National Technical University
64 Zhukovsky Str., 69063, Zaporozhye, Ukraine. E-mail: rector@zntu.edu.ua
[2]LLC «Paton Turbine Technologies»
26 Raketnaya Str., 036028, Kiev, Ukraine. E-mail: VKurenkova@patontt.com

According to the algorithm of a developed comprehensive analytical solution method (CASM), a new cast high-temperature corrosion-resistant nickel alloy ZhS3LS-M has been developed for manufacture of all-cast nozzle appliances. The developed alloy is characterized by the high-temperature strength σ_{40}^{975} = 180–200 MPa at the level of the industrial non-corrosion-resistant alloy VZhL12E as well as technological weldability and corrosion resistance at the level of commercial weldable corrosion-resistant alloy ZhS3LS. 24 Ref., 11 Tables, 1 Figure.

Keywords: *cast high-temperature nickel alloys; performance parameters; CASM-method; regression model; regression equation; service properties, technological weldability*

At present time application of new high-temperature materials and technologies of manufacture of the parts for gas turbine engines (GTE) allows providing a high level of requirements to perspective GTE. Therefore, one of the progressive directions of increase of service characteristics of GTE critical parts is getting the all-cast nozzle appliances (NA) form new cast corrosion-resistant high-temperature nickel alloys (HNA) characterized simultaneously by technological weldability and increased strength characteristics [1–6].

Commercial alloys ZhS3LS and VZhL12E are referred to the most well-known cast HNA widely used for manufacture of all-cast NA of different type. VZhL12E alloy, doped with aluminum in 5.0–5.7 wt.% quantity, in which volume fraction of γ′-phase reaches 58–62 %, has increased thermal stability of structural-phase composition. This provides higher high-temperature strength and better resistance to high-temperature material creep up to 1000 °C in comparison with ZhS3LS alloy, doped with aluminum in 2.4–3.0 wt.% quantity, in which volume fraction of γ′-phase makes only 38–42 %. However, VZhL12E alloy is not characterized by good technological weldability and necessary corrosion resistance that makes its further application not so perspective. The indicated characteristics are typical for commercial alloy ZhS3LS, however, it doesn't have necessary level of strength, that also limits its application for perspective GTE [6–11].

© S.V. GAJDUK, V.V. KONONOV and V.V. KURENKOVA, 2017

Respectively, designing and implementation into industry of new cast corrosion-resistant HNA differ by technological weldability and increased level of high-temperature strength, is a relevant, competitive and economically profitable direction for manufacture of all-cast nozzle appliances of perspective GTE using a developed express computer designing method replacing low-effective empirical trial and error method.

Problem statement. Welding/surfacing of high-temperature nickel alloys is sufficiently complex process due to presence in them of large quantity of main strengthening γ′-phase — Ni_3Al (more than 60 vol.%). In particular, precipitations of this phase in process of solidification or further heat treatment results in appearance of dispersion hardening cracks [11] in the welds or heat-affected zones.

Aim of the present work is designing employing developed express comprehensive analytical solution method (CASM) [12] of a new cast corrosion-resistant HNA for manufacture of all-cast nozzle appliances (NA) of different types, differ by technological weldability at the level of commercial alloy ZhS3LS and increased strength characteristics at the level of non-weldable and non-corrosion-resistant commercial alloy VZhL12E.

A search of perspective compositions of the developed alloy was carried out according to the algorithm of computer modelling by CASM based on a doping system of commercial cast corrosion-resistant nickel alloy ZhS3LS taken as a prototype. Chemical com-

Table 1. Composition (wt.%) of commercial cast nickel alloys ZhS3L and VZhL12E of average doping level [6. 10]

Alloy grade	C	Cr	Co	Mo	W	Al	Ti	Nb	V	Zr	B	Ni
ZhS3LS	0.09	16.0	5.0	4.0	4.0	2.7	2.7	–	–	0.015	0.015	Base
VZhL12E	0.16	9.25	9.0	3.1	1.4	5.4	4.5	0.75	0.75	0.020	0.015	Base

position of the latter is given in Table 1 together with composition of commercial high-temperature alloy VZhL12E taken as an analogue.

New elements such as hafnium and tantalum were introduced in the selected basic doping system of alloy ZhS3LS (Ni–Co–Cr–Al–Ti–Mo–W–Zr–B–C) for the following reasons:

- tantalum and hafnium promote increase of volume fraction of main γ′-phase and rise of its thermal-dynamic stability;
- have positive effect on morphology of carbide phase of MeC type, at that obviously suppress a mechanism of formation of less thermodynamically stable and unfavorable on morphology carbides of $Me_{23}C_6$ type, that promotes rise of material ductility factor;
- promote significant increase of temperature of complete solution of main strengthening γ′-phase, and, respectively, rise of its residual quantity at high temperatures, that guarantees increase of high-temperature strength characteristics, and, respectively, long-term strength.

Based on mentioned above, the initial conditions for alloy designing in a new system of multicomponent doping Ni–Co–Cr–Al–Ti–Mo–W–Ta–Hf–Zr–B–C were formulated. The main controlled parameters, introduced into computation for multicriterial optimization of composition of developed alloy, are given below.

Stability parameter
P_{TCP} = % Cr/%[Cr + Mo + W] . . . . . 0.825±0.025
Total number of electron vacancies in γ-solid solution N_{v_γ} 2.40
Total number of valence electrons in γ-solid solution M_{d_γ} 0.93
Total number of valence electrons in alloy M_{d_C} . . . . . 0.980±0.008
Parameter of disbalance of doping system ΔE . . . . . ±0.04
Total content $\sum_\gamma$ = (Mo + W + Ta + Re + Ru), wt.% . . . . . ≥10.0
Total content $\sum_{\gamma'}$ = (Al + Ti + Nb + Ta + Hf), wt.% . . . . . $8.0 < \sum_{\gamma'} < 9.0$
Solidus temperature t_S °C . . . . . ≥1280
Temperature interval of homogenization Δt_{hom}, °C . . . . . ≥20
Quantity of strengthening γ′-phase (20 °C) $V_{\gamma'}^{20}$, vol.% . . . . . $43 < V_{\gamma'}^{20} < 50$
Dimensional mismatch of γ and γ′-lattices (misfit) . . . 0.15–0.45
Short-term strength limit (20 °C) σ_t^{20}, MPa . . . . . ≥850
Relative elongation (20 °C) δ^{20}, %. . . . . ≥5.0
Long-term strength $\tau_{fract}\ \sigma_{180}^{975}$, h . . . . . ≥40
Corrosion parameter P_{CR} = √% Cr % [Ti/Al] . . . . . ≥3.0
Critical temperature of accelerated HTC, t_{crit}, °C . . . . . ≥800
Removal of cast defects in all-cast NA by argon-arc welding (AAW) method . . . . . Technological weldability at the level of ZhS3LS alloy

Analysis of the results. This work presents the results of computer designing and experimental investigations of new cast corrosion-resistant nickel alloy designed for manufacture of all-cast NA of TVZ-117 type under conditions of commercial enterprise V.I. Omelchenko ZMZ, having increased strength characteristics and technological weldability. In contrast to more high-temperature commercial alloy VZhL12E, containing 9 wt.% of Cr and does not differ by good corrosion resistance, commercial weldable corrosion-resistant alloy ZhS3LS contains larger quantity of chromium (16 wt.%). In turn, ZhS3LS alloy does not have necessary level of high-temperature strength since quantity of main strengthening γ′-phase makes only 38–42 % that is 20 % lower than in VZhL12E alloy (58–62 %). Therefore, the following requirements were formulated for multicriterial optimization of composition of developed alloy and main controlled parameters, being entered in a complex computation, were selected:

- fulfillment of the conditions of structural stability by parameters: P_{TCP} = % Cr/%(Cr + Mo + W) = = 0.825±0.025;
- $N_{v_\gamma} \le 2.40$; $M_{d_\gamma} \le 0.93$; ΔE = ±0.04; M_{d_C} = = 0.980±0.008;
- providing technological weldability at the level of ZhS3LS alloy, taken as a prototype, as well as strength characteristics close to the level of commercial cast high-temperature alloy VZhL12E, taken as an analogue: controlled quantity of main strengthening γ′-phase within the limits of $43 < V_{\gamma'}^{20} < 50$ % (on mass): short-term strength $\sigma_t^{20} \ge 850$ MPa; $\delta^{20} \ge$ ≥ 5.0 % and long-term strength $\sigma_{180}^{975} \ge 40$ h in accordance with OST 1.90126–85;
- providing corrosion resistance at the level of commercial cast corrosion-resistant alloy ZhS3LS, taken as a prototype: corrosion parameter P_{cr} = %(Ti/Al) ≥ 3.0.

Indicated above values of characteristics for developed alloy were obtained of multicriterial optimization of the composition doped with hafnium and tantalum based on commercial alloy ZhS3LS employing an algorithm of developed CASM express-method (Figure). The following approaches can be referred to conceptually new approach in balancing of doped cast HNA:

- in order to provide serviceability of developed alloy it is necessary to balance general chemical composition of the alloy: by γ′-forming elements with-

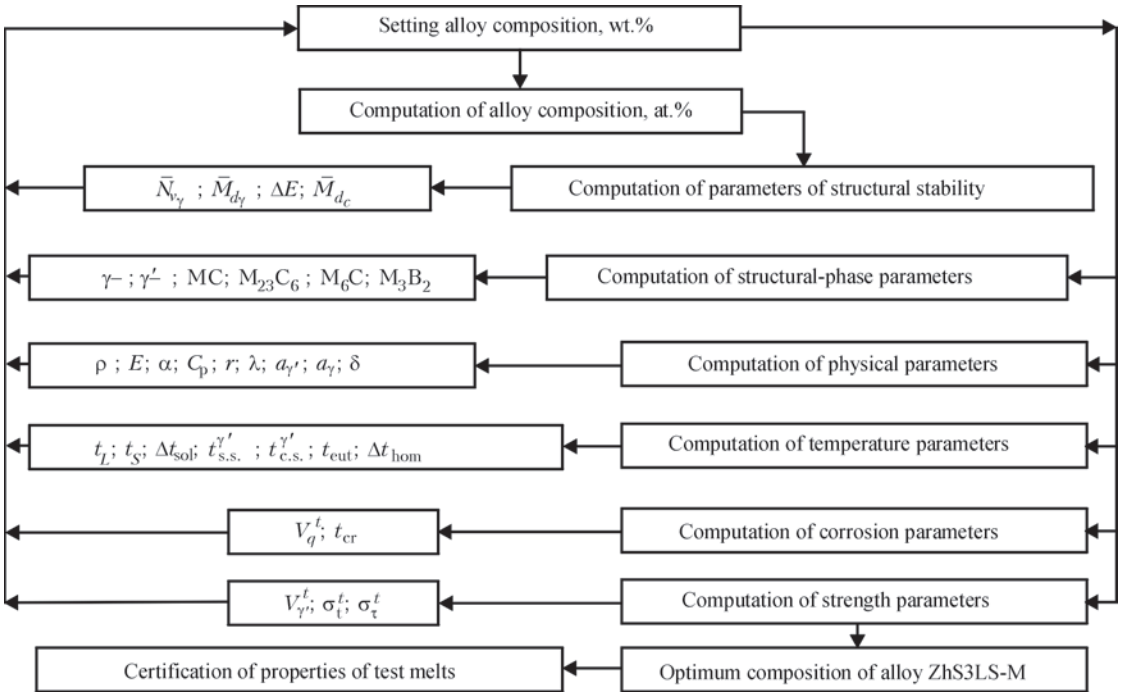

Algorithm of computer computation of designed alloy ZhS3LS-M on developed CRAM method [12]

in the limits of $\Sigma_{\gamma'}$ = %(Al + Ti + Nb + Ta + Hf) = = 8–9 wt.%; by elements strengthening γ-solid solution Σ_γ = %(Mo + W + Ta + Re + Ru) ≥ 10 wt.%

● in order to provide the required level of strength characteristics it is necessary to increase the value of misfit factor δ due to rise of the size mismatch of periods of crystalline lattices of γ′-phase and γ-solid solution. It can be reached by introduction of the optimum quantity of hafnium and tantalum in a new doping system of the developed alloy. They have positive effect on misfit factor value;

● introduction of the optimum quantity of hafnium (0.3 wt.%) and tantalum (2.5 wt.%) in doping system of the designed alloy at decrease of chromium from 16 to 14.5 % as well as increase of doping lower boundary on aluminum from 2.5 to 3.2 % and on tungsten from 3.5 to 6.2 % in the basic doping system of ZhS3LS alloy as well as decrease of doping upper boundary on molybdenum from 4.5 to 2.5 wt.%. This guarantees necessary level of technological and corrosion characteristics in rise of temperature level of strength characteristics.

The following variable doping elements were selected as alternating factors for the investigated computed compositions, namely hafnium and tantalum as well as elements included in the composition of basic alloy ZhS3LS, i.e. chromium, tungsten and molybdenum. A range of variation of concentration of investigated doping elements in the selected new doping system Ni–Co–Cr–Al–Ti–Mo–W–Ta–Hf–Zr–B–C was set in the following limits, wt.%: 0–0.5 Hf; 0–3.5 Ta; 4.0–7.5 W; 1.0–4.0 Mo; 3.5–16.0 Cr.

Initially, a computer experiment was used to carry an evaluation of structural stability of the computed compositions in a set range of variation by indicated elements on N_{v_γ}, M_{d_γ}, M_{d_C} and ΔE parameters using traditional methods following known regression equations (RE) [1–4, 6, 7, 13–20] as well as mathematical regression models (RM) in accordance with the algorithm (see Figure) of developed CASM method [12, 21–24].

It is known [1, 2, 14–17] that the value and sign of parameter of doping disbalance ΔE determines a direction of the reactions in γ-solid solution and tendency of high-temperature nickel alloys to precipitation of that or another type of TCP (topologically close-packed) phases. Thus, the alloys with large negative doping disbalance (ΔE < –0.04) have high probability to formation of heterotypical compounds, i.e. carbides of M_6C type, α-phases based on vanadium and molybdenum as well as topologically close-packed phases of σ, μ type. The alloys with large positive doping disbalance (ΔE < 0.04) are susceptible to formation of homeotypic compounds of η-phase type based on Ni_3Ti, Ni_3Nb, Ni_3Ta as well as eutectic (peritectical) phases based on Ni_3Al. If ΔE = 0 than the alloy composition is supposed to be ideally balanced.

Table 2 represents the pilot variants of compositions 1–5 of designed alloy together with compositions of commercial alloys ZhS3LS and VZhL12E of medium doping level. Mixtures of the compositions, which satisfy the conditions: P_{TCP} = 0.80–0.85; $N_{v_\gamma} \leq$ ≤ 2.40 and $M_{d_\gamma} \leq 0.93$; –0,04 < ΔE < 0.04 and 0.972 ≤ ≤ M_{d_C} < 0.988, supposed to be phase stable.

Table 2. Effect of doping elements of basic composition of commercial alloy ZhS3LS on parameters of its structural stability

Composition number	Content of elements, wt.%				Quantity of γ'-phase, vol.%	Misfit, %	Structural stability parameters				
	Hf	Ta	Cr	W/Mo	$V_{\gamma'}^{20}$	δ	P_{TCP}	N_{v_γ}	M_{d_γ}	M_{d_C}	ΔE
ZhS3LS	–	–	16.0	1.00	40.6	0.171	0.8290	2.2141	0.9100	1.0061	0.1372
1	0.1	1.5	15.5	1.83	45.9	0.290	0.8297	2.2597	0.9144	0.9857	0.0289
2	0.2	2.0	15.0	2.40	47.2	0.338	0.8309	2.2593	0.9143	0.9850	0.0250
3	0.3	2.5	14.5	3.25	48.6	0.377	0.8322	2.2566	0.9141	0.9840	0.0200
4	0.4	3.0	14.0	4.67	50.0	0.404	0.8337	2.2510	0.9134	0.9832	0.0156
5	0.5	3.5	13.5	7.50	51.3	0.412	0.8352	2.2489	0.9134	0.9824	0.0111
VZhL12E	–	–	9.25	0.45	60.8	0.151	0.8172	2.2287	0.9114	0.9847	0.0235

Table 3. Parameters of structural stability of ZhS3LS-M alloy [21]

Computation method	Structural stability parameters				
	P_{TCP} = = 0.825±0.025	$N_{v_\gamma} \le 2.40$	$M_{d_\gamma} \le 0.93$	ΔE = ±0.04	M_{d_C} = = 0.980±0.008
RE	–	2.1945	0.9049	0.0200	0.9692
RM	0.8323	2.2566	0.9141	0.0200	0.9840

Table 4. Values of structural-phase parameters of alloy ZhS3LS-M [24]

Phase type	Phase quantity, vol.%		CALPHAD-method [24]											
			Computed composition of phases at 20 °C, wt.%											
	Experiment	Computation	C	Co	Cr	Al	Ti	Mo	W	Ta	Hf	Zr	B	Ni
γ-	49.3–48.15	48.94	–	7.95	25.3	0.38	0.06	1.4	5.67	0.14	–	–	–	59.1
γ′-	48.5–49.5	48.6	–	1.67	1.88	5.83	6.12	0.13	4.11	5.01	0.62	0.03	–	74.6
MC	0.95–1.05	1.03	10.1	–	0.63	–	25.8	0.49	9.75	37.9	15.1	0.23	–	–
$M_{23}C_6$	1.25–1.30	1.25	5.16	0.77	71.7	–	–	18.1	1.43	–	–	–	–	2.84
M_3B_2	Not found	0.18	–	–	20.7	–	–	69.5	1.65	–	–	–	8.15	–

Table 5. Values of physical parameters of alloy ZhS3LS-M

Alloy ZhS3LS-M	Physical parameters at 20 °C [24]								
	ρ	E	$\alpha \cdot 10^6$	C_p	$r \cdot 10^6$	λ	$a_{\gamma'} \cdot 10^{-4}$	$a_{\gamma'} \cdot 10^{-4}$	δ
Unit	g/cm³	GPa	1/K	J/g·K	Ohm·m	W/m·K	μm	μm	%
CALPHAD	8.47	213.25	11.46	0.42	0.71	10.29	3.589	3.575	0.377

Note. ρ is the specific density; E is the Young's modulus; α is the coefficient of thermal expansion; C_p is the specific heat; r is the specific electric resistance; λ is the heat conduction; $\alpha_{\gamma'}$ is the parameters crystalline lattice of γ′-phase; α_γ is the parameters crystalline lattice of γ-solid solution; δ is the size mismatch of lattice parameters (misfit).

Table 6. Temperature parameters of alloy ZhS3LS-M [12, 22]

Evaluation method	$\sum_\gamma$	t_L	t_S	$\sum_{\gamma'}$	t_{eut}	$t_{s.s.}^{\gamma'}$	$t_{c.s.}^{\gamma'}$	Δt_{cr}	Δt_{hom}	t_{hom}
Computation on RM	11.0	1370	1286	8.8	1243	845	1176	84	67	–
Experiment	–	1355	1290	–	1220	–	1160	65	60	1190

Note. Σ_γ is the total content of elements, strengthening γ-solid solution; $\Sigma_{\gamma'}$ is the total content of elements stabilizing γ′-phase; t_L is the liquidus temperature; t_S is the solidus temperature; t_{eut} is the temperature of local melting of eutectic γ′-phase; $t_{s.s.}^{\gamma'}$, $t_{c.s.}^{\gamma'}$ are the temperatures of start and complete (end) solution of γ′-phase; Δt_{sol} is the interval of alloy solidification; Δt_{hom} is the temperature interval for homogenization; t_{hom} is the optimum temperature for alloy homogenization.

Table 7. Characteristics of ZhS3LS-M alloy corrosion [12, 23]

Evaluation method	V_q^t, g/(m²·s)					
	$P_{cr} \geq 3{,}0$	$V_q^{800} \cdot 10^3$	$V_q^{850} \cdot 10^3$	$V_q^{900} \cdot 10^3$	$V_q^{950} \cdot 10^3$	t_{cr}, °C
Computation of RM	3.81	0.0483	0.9719	3.5846	6.0234	817
Experiment	–	0.04	0.90	3.50	5.90	820

Computations of parameters of structural stability such as N_{v_γ}, M_{d_γ}, ΔE, M_{d_C} were carried out by means of transfer of compositions of γ-solid solutions and general compositions in at.%.

Table 2 shows that pilot compositions 1–5 as well as commercial alloy VZhL12E are balanced from point of view of conditions of doping disbalance $\Delta E = \pm 0.04$. The value of disbalance of doping system ΔE in the pilot compositions 1–5 is in the limits from 0.0111 to 0.0289 that satisfies the conditions of balanced doping. It should be noted that the value of imbalance of the doping system of basic commercial alloy ZhS3LS, taken as a prototype, does not satisfy the conditions of balanced doping of chemical composition ($\Delta E = 0.1372$). At that ZhS3LS alloy is technologically weldable since quantity of main strengthening γ′-phase corresponds to the condition ($V_{\gamma'}^{20}$ = = 40.6–50 %) in contrast to more high-temperature alloy VZhL12E ($V_{\gamma'}^{20}$ = 60.8 %), which is not characterized by good technological weldability. At the same time ZhS3LS alloy does not have necessary level of high-temperature strength since quantity of main strengthening γ′-phase does not correspond to $43 \leq V_{\gamma'}^{20} \leq 50$ % condition.

Further in accordance with the algorithm of CASM method (see Figure) structural-phase, physical, temperature, corrosion and strength groups of parameters were calculated for the phase-stable compositions 1–4.

In selection of optimum composition of designed alloy for manufacture of all-cast NA, differing by technological weldability, it is shown that structural stability is the necessary, but insufficient condition for getting required indices of high-temperature strength. The necessary structural and physical factors, providing the required level of high-temperature strength in 800–1000 °C temperature interval, are the value of volume fraction of γ′-phase, which should lie in the controlled limits ($43 \leq V_{\gamma'}^{20} \leq 50$ %) on mass as well as misfit-factor, value of which should lie in ($0.15 < \delta < 0.45$ %) limits.

Pilot composition 3 (see Table 2), with assigned designation of ZhS3LS-M grade, was selected for further experimental investigations taking into account a comparative analysis of received data on groups of computed characteristics for pilot compositions, by means of multicriterial optimization of the composition on controlled parameters.

Experimental investigations were carried out on the pilot specimens of test melts by set parameters in accordance with Table 2.

The optimized composition of designed alloy ZhS3LS-M was the following, wt.%: 0.10 C; 14.5 Cr; 4.5 Co; 3.0 Al; 3.0 Ti; 6.5 W; 2.0 Mo; 2,5 Ta; 0.3 Hf; 0.015 Zr; 0.015 B; Ni — base.

Comparative assessment of a tendency to structural and phase instability of the optimized composition of designed alloy ZhS3LS was carried out using

Table 8. Quantity of γ′-phase in ZhS3LS-M alloy, vol.% [12, 24]

Evaluation method	$V_{\gamma'}^{20}$	$V_{\gamma'}^{800}$	$V_{\gamma'}^{900}$	$V_{\gamma'}^{1000}$
Computation of RM	48.6	47.5	44.6	33.9
Experiment	48.9	–	–	–

Table 9. Characteristics of short-term strength of alloy ZhS3LS-M, MPa [12, 24]

Alloy ZhS3LS-M	σ_t^{20}	σ_t^{800}	σ_t^{900}	σ_t^{1000}	δ^{20}	δ^{800}	δ^{900}	δ^{1000}
Computation of RM	979	835	860	502	–	–	–	–
Experiment	930–975	811–836	849–854	500–563	8.8–13.2	3.8–5.3	2.9–5.9	5.0–11.8

Table 10. Long-term strength limit (100 and 1000 h) of alloy ZhS3LS-M, MPa [12, 24]

Alloy ZhS3LS-M	σ_{100}^{800}	σ_{1000}^{800}	σ_{100}^{900}	σ_{1000}^{900}	σ_{100}^{1000}	σ_{1000}^{1000}
Computation of RM	480	370	280	180	120	70
Experiment	480–500	350–370	280–300	170–190	110–130	70–80

Table 11. Comparative values of alloy characteristics

Characteristics of parameters by groups	Values of alloy characteristics		
	Alloy-prototype ZhS3LS	Designed alloy ZhS3LS-M	Alloy-analogue VZhL12E
Parameters of structural stability			
$P_{TCP} = 0.825 \pm 0.025$	0.8290	0.8323	0.8175
$N_{\gamma} \leq 2.40$	2.2141	2.2566	2.2287
$M_{d_\gamma} \leq 0.93$	0.9100	0.9141	0.9114
$M_{d_C} = 0.980 \pm 0.008$	0.1372	0.0200	0.0235
$\Delta E = \pm 0.04$	0.1372	0.0200	0.0235
Structural-phase parameters			
$43 \leq V_{\gamma'} \leq 50$, vol.%	38.0–42.0	43.5–49.5	58.0–62.0
Physical parameters			
ρ, g/cm^3	8.33	8.47	7.93
misfit $0.15 \leq \delta \leq 0.45$ %	0.171	0.377	0.151
Temperature characteristics			
t_L, °C	1354	1355	1334
$t_{Sol} \leq 1280$, °C	1260	1290	1273
Δt_{cr}, °C	94	65	61
$t_{eut.}$, °C	1188	1220	1229
$t^{\gamma'}_{s.s.}$, °C	835	850	851
$t^{\gamma'}_{c.s.}$, °C	1090	1160	1222
Δt_{hom}, °C	98	60	7
T_{hom}, °C	1150±10	1190±10	Withou HT
Corrosion resistance parameters			
$P_{CR} \cdot 3.0$	4.00	3.81	2.53
$V_q^{800} \cdot 10^3$, g/(m^2·s)	0.04	0.05	0.16
$V_q^{850} \cdot 10^3$, g/(m^2·s)	0.82	0.97	2.98
$V_q^{900} \cdot 10^3$, g/(m^2·s)	3.07	3.58	9.97
$V_q^{950} \cdot 10^3$, g/(m^2·s)	5.24	5.92	15.12
t_{cr}, °C	825	820	770
Mechanical parameters			
Short-term strength:			
$\sigma_t^{20} \geq 850$ MPa	740–70	930–975	910–975
σ_t^{800}, MPa	620–650	911–956	880–1000
σ_t^{900}, MPa	520–600	849–854	850–870
σ_t^{1000}, MPa	–	500–563	500–580
Long-term strength:			
σ_{100}^{800}, MPa	380–400	480–500	480–530
σ_{1000}^{800}, MPa	–	350–370	370–420
σ_{100}^{900}, MPa	180–200	280–300	270–305
σ_{100}^{900}, MPa	–	170–90	180–205
σ_{100}^{1000}, MPa	–	110–130	120–145
σ_{1000}^{1000}, MPa	–	70–80	75–90
$\sigma_{260}^{975} \geq 40$ h	–	44–68	68–127
Elimination of cast defects in all-cast NA by AAW method	Differs by technological weldability	Differs by technological weldability	Not characterized by technological weldability

traditional computation methods PHACOMP (N_v) [7, 11], New PHACOMP (M_d) [13], ΔE-method [14–17] with their known regression equations (RE) as well as received mathematical regression models (RM) [12, 21–24] (Table 3).

Computations using CALPHAD method [25] on structural-phase and physical parameters [24, 26] were carried out based on criteria (parameters) of serviceability of cast HNA, grounded on works [12, 21–24]. Tables 4 and 5 represent the computed values of structural-phase and physical parameters for designed alloy ZhS3LS-M of the optimum doping level.

Table 6 represents the computed and experimental values, which were received by a method of differential thermal analysis (DTA) on VDTA-8M unit in helium at constant heating rate (cooling) being equal 80 °C/min. Thermally inert specimen of pure tungsten (W-reference) was used as a reference. Calibration technology on temperatures of melting of pure metals allowed getting well reproducible results independent on heating rate.

A complex of comparative experimental investigations was carried out on pilot specimens of test melts from designed alloy ZhS3LS-M in comparison with the similar specimens of commercial alloys ZhS3LS and VZhL12E. The pilot specimens of designed alloy ZhS3LS-M were received using vacuum-induction melting on unit of UPPF-3M type by series technology.

Computation investigations of (high temperature corrosion) HTC-resistance were carried out for composition of designed alloy ZhS3LS-M (Table 4) in synthetic ash at testing temperatures 800, 850, 900 and 950 °C on the basis of 100 h following received mathematical RM for given group of parameters [12, 23]. Experimental investigations of HTC-resistance of the specimens of test melt of alloy ZhS3LS-M were carried out in synthetic ash at testing temperatures 800, 850, 900 and 950 °C in comparison with alloys ZhS3LS and VZhL12E using method developed by Nikitin V.I. (I.I. Polsunov CBTI), which is widely applied in the field [8–10]. The experiments at all temperatures were carried out during 100 h. Resistance of specimens of pilot compositions to HTC was evaluated on average corrosion rate V_q^t g/(m²·s). Table 7 represents the computed and experimental values of corrosion parameters of designed alloy ZhS3LS-M.

Mechanical tests for short-term and long-term strength were carried out on the standard cylinder specimens from developed alloy ZhS3LS-M using standard procedures. Short-term strength tests were performed at 20, 800, 900 and 1000 °C temperatures on tensile-testing machines UME-10TM and GSM-20 (GOST 1497–61, GOST 9651–73 and GOST 1497–84). Long-term strength tests were carried out at 800, 900, 975 and 1000 °C temperature on AIMA-5-2 and ZTZ 3/3 machines (GOST 10145–81). Quantity of γ´-phase in ZhS3LS-M alloy is presented in Table 8.

Tables 9 and 10 show the computed and experimental values of limits of short-term and long-term strength of the specimens of test melts of designed alloy ZhS3LS-M at different temperatures.

Table 11 gives the comparative results of computed and experimental values of characteristics of designed alloy ZhS3LS-M on groups of parameters, namely structural stability, structural-phase, physical, temperature, corrosion and strength characteristics in comparison with the values of similar characteristics of commercial alloys ZhS3LS and VZhL12E.

It is determined as a result of multicriterial optimization of composition based on computation and experimental investigations of set design conditions that developed alloy ZhS3LS-M provides necessary level of required parameters and characteristics. The balanced composition with indicated doping limits contains the optimum quantity of tantalum — 2.5±0.3 wt.%; lower content of chromium — 14.5±0.3 wt.%, molybdenum — 2.0±0.5 wt.% and higher content of tungsten — 6.5±0.3 wt.% than in commercial alloy ZhS3LS, taken as a prototype; lower content of aluminum — 3.3±0.3 wt.% than in VZhL12E alloy, taken as an analogue.

5 melts from developed alloy ZhS3LS-M of total mass 500 kg were certified by strength characteristics under production conditions of JSC «Motor Sich». The pilot all-cast nozzle apparatus SA TVZ-117 were manufactured by serial technology under production conditions of V.I. Omelchenko ZMBP enterprise. Technological process of elimination of the cast defects by AAW method was modernized. Pilot SA TVZ-117 was installed on technological engine, where it has worked for a period of service life with a positive result and is working up to the moment in order to increase specified service life.

Conclusions

1. Multicriterial optimization of composition on algorithm of developed CASM method allowed designing a new cast weldable corrosion-resistant alloy ZhS3LS-M for manufacture of all-cast NA of different types a varying by increased strength characteristics at the level of high-temperature non-weldable and non-corrosion-resistant alloy VZhL12E as well as characterizing with corrosion resistance and technological weldability at the level of commercial cast weldable corrosion-resistant nickel alloy ZhS3LS.

2. New developed alloy ZhS3LS-M is implemented in commercial production of JSC «Motor Sich» for manufacture of all-cast nozzle apparatus of TVZ-117

type of different stages instead of widely used commercial alloys ZhS3LS and VZhL12E.

1. Kablov, E.N. (2006) Cast high-temperature alloys. S.T. Kiskin effect. In: *Transact. to 100th Anniversary of S.T. Kishkin*. Ed. by Kablov. Moscow, Nauka [in Russian].
2. Kablov, E.N. (2007) 75 years. Aviation materials. *Selected works of VIAM: Jubelee Sci.-Techn. Transact*. Ed. by E.N. Kablov. Moscow, VIAM [in Russian].
3. Shalin, R.E., Svetlov, I.L., Kachanov, E.B. et al. (1997) *Single crystals of nickel high-temperature alloys*. Moscow, Mashinostroenie [in Russian].
4. Kishkin, S.T., Stroganov, G.B., Logunov, A.V. (1987) *Cast high-temperature nickel-base alloys*. Moscow, Mashinostroenie [in Russian].
5. Paton, B.E., Stroganov, G.B., Kishkin, S.T. et al. (1987) *High-temperature strength of cast nickel alloys and their protection from oxidation*. Kiev, Naukova Dumka [in Russian].
6. Kablov, E.N. (2001) *Cast blades of gas-turbine engines (alloys, technology, coatings)*: State Scientific Center of Russian Federation. Moscow, MISIS [in Russian].
7. Sims, Ch.T., Stoloff, N.S., Hagel, U.K. (1995) *Superalloys II*: High-temperature materials for aerospace and industrial power units. Ed. by R.E. Shalin. Moscow, Metallurgiya [in Russian].
8. Koval, A.D., Belikov, S.B., Sanchugov, E.L., Andrienko, A.G. (1990) *Scientific basics of alloying of high-temperature nickel alloys resistant to high-temperature corrosion (HTC)*. Zaporozhye Machine Building Institute [in Russian].
9. Nikitin, V.I. (1987) *Corrosion and protection of gas turbine blades*. Leningrad, Mashinostroenie [in Russian].
10. Khimushin, F.F. (1969) *High-temperature alloys*. Moscow, Metallurgiya [in Russian].
11. Du Pont, J.N., Lippold, J.C., Kiser, S.D. (2009) *Welding metallurgy and weldability of nickel-base alloys*. New Jersey, 298–326.
12. Gajduk, S.V. (2015) Comprehensive analytical solution method procedure for design of cast high-temperature nickel-base alloys. *Novi Materialy i Tekhnologii v Metalurgii ta Mashynobuduvanni*, **2**, 92–103 [in Russian].
13. Morinaga, M., Yukawa, N., Adachi, H., Ezaki, H. (1984) New PHACOMP and its application to alloy design. *Superalloys, AIME*, 523–532.
14. Morozova, G.I. (2012) Compensation of disbalance of alloying of high-temperature nickel alloys. *Metallovedenie i Termich. Obrab. Metallov*, **12**, 52–56 [in Russian].
15. Morozova, G.I. (1993) Balanced alloying of high-temperature nickel alloys. *Metally*, **1**, 38–41 [in Russian].
16. Gajduk, S.V., Tikhomirova, T.V. (2015) Application of analytical methods for calculation of chemical composition of γ-, γ´-phases and parameters of phase stability of cast high-temperature nickel alloys. *Aviats.-Kosmich. Tekhnika i Tekhnologiya*, 126(**9**), 33–37[in Russian].
17. Gajduk, S.V., Kononov, V.V., Kurenkova, V.V. (2015) Construction of predictive mathematical models for calculation of thermodynamical parameters of cast high-temperature nickel alloys. *Sovrem. Elektrometall*., **4**, 31–37 [in Russian].
18. Gajduk, S.V., Kononov, V.V., Kurenkova, V.V. (2016) Regression models for predictive calculations of corrosion parameters of cast high-temperature nickel alloys. *Ibid*., **3**, 51–56 [in Russian].
19. Gajduk, S.V., Tikhomirova, T.V. (2015) Application of CALPHAD method for calculation of γ'- phase and prediction of long-term strength of cast high-temperature nickel alloys. *Metallurg. i Gornorudnaya Promyshlennost*, **6**, 64–68 [in Russian].
20. Saunders, N., Fahrmann, M., Small, C.J. (2000) The application of CALPHAD calculations to Ni-based superalloys. In: *Superalloys 200*0. TMS, Warrendale, 803–811.
21. Gajduk, S.V., Kononov, V.V., Kurenkova, V.V. (2015) Calculation of phase composition of cast high-temperature corrosion-resistant nickel alloy by CALPHAD method. *Sovrem. Elektrometall*., **3**, 35–40 [in Russian].
22. Vertogradsky, V.A., Rykova, T.P. (1984) Investigation of phase transformations in alloys of high-temperature type by DTA method. In: *High-temperature and heat-resistant nickel-base steels and alloys*. Moscow, Nauka, 223–227 [in Russian].
23. Gajduk, S.V., Belikov, S.B., Kononov, V.V. (2004) About influence of tantalum on characteristic points of high-temperature nickel alloys. *Vestnik Dvigatelestroeniya*, **3**, 99–102 [in Russian].
24. Gajduk, S.V., Petrik, I.A., Kononov, V.V. (2015) Comparative investigations of weldability of cast high-temperature nickel alloys. *Novi Materialy i Tekhnologii v Metalurgii ta Mashynobuduvanni*, **1**, 82–88 [in Russian].

Received 22.11.2017

doi.org/10.15407/tpwj2017.12.02

STUDY OF PROPERTIES OF WELDED JOINT USING DANTEC'S ISTRA 4D SYSTEMS*

T. DOMAŃSKI, W. PIEKARSKA and **M. KUBIAK**
Czestochowa University of Technology
Generala I.N. Dabrowskiego 69, 42-201, Czestochowa, Poland. E-mail:domanski@imipkm.pcz.pl

The paper presents displacement and strain fields measured at various stages of tension of flat samples in order to compare the effect of different technological parameters on mechanical properties of welded joints. Results of measurements are also compared with the results of tensile test of the base material to determine the impact of welding process on changes of mechanical properties of tested steel. The measurement of displacements and strains in tensed flat specimens made of S355 steel, hybrid welded using electric arc and laser beam is in the scope of this work. Welding process is performed using Yb:YAG laser and electric arc in GMAW method. D70 Trumpf laser head with maximum power up to 12 kW is used in welding tests with a spot diameter of the laser beam d = 0.8 mm. Welded joints are made for different technological parameters of the process with laser beam heat source leading in the tandem. Tension tests of flat samples are performed in accordance with norm PN-EN ISO 6892-1. Dantec Q-400 ISTRA multi-camera 3D correlation system is used for strain and displacement measurements. The method of measurement is based on the correlation of digital images recorded by the three cameras. Surface of tested samples is covered with a layer of white and black paint. The measurement took place by tracking movements of spots covering the surface of the sample, loaded by longitudinal force. 6 Ref., 4 Figures.

Keywords: *hybrid welding, electric arc, laser, welded joints, mechanical properties, tensile tests, deformation fields*

Today's facilities are characterized by high functional diversity, which, while maintaining high quality of workmanship, is very difficult. Products are increasingly demanding, and consequently products have increasingly complex 3D geometry. Measurement tools should combine the speed of collection of measurement points with high accuracy. The use of a non-invasive measurement method makes it possible to detect defects much faster without the need for specialist preparation of test specimens [1–3]. Coupled thermal, structural and mechanical phenomena occurring in welding process have a direct impact on the quality of welded joint. The material in the weld and adjacent region is heated to various temperatures resulting in a variety of structures that occur in the joint and heat affected zone (HAZ), having different mechanical properties in comparison to base material. Theoretical and experimental analysis of mechanical behaviour of welded joint is still one of the fundamental industrial problems. In the welding process using a laser beam a high welding speeds are obtained with a good quality of welds and a narrow thermal influence zone which is helpful in increasing the quality and mechanical properties of the joint as well as the production efficiency. One of the modern welding technologies is laser-arc hybrid welding, which combines laser beam welding with classical electric arc welding cooperating in a single process. This method has many advantages in comparison to welding process with electric arc or laser beam heat sources used separately. Advantages of laser-arc hybrid welding process include higher welding stability, higher melting efficiency, easier input of additional material to the welding pool and a lower input power under the same welding penetration. The investigations about laser-arc hybrid welded steel have been reported widely and applied successfully in a wide range of the industry. These studies include analytical modeling of thermomechanical phenomena occurring in the process and experimental research on plasma formation, liquid material flow through the welding pool, microstructure composition as well as the analysis of welding deformations and mechanical properties of welded joints, performed in both destructive and nondestructive tests. One of usually performed tests on welded joints is the classical tension test. The standard for this type of testing is the norm

*By materials of a report made at VIII International Conference on «Beam Technologies in Welding and Materials Processing», September 10–16, 2017, Odessa.

© T. DOMAŃSKI, W. PIEKARSKA and M. KUBIAK, 2017

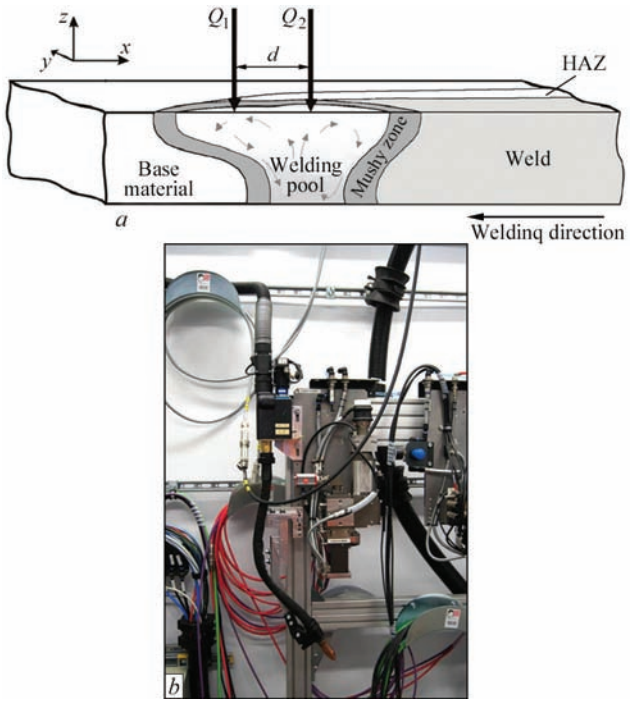

Figure 1. Scheme of hybrid welding process (*a*), hybrid laser head Yb: YAG + MIG (*b*)

PN-EN ISO 6892-1. This test allows the determination of basic mechanical properties of welded joints. However, the development in new measurement systems, such as 3D multicamera correlation system allows the analysis of deformations at the surface area of tensed sample in control area determined for cameras used in the experiment. The knowledge about strain distribution in the joint combined with the analysis of the microstructure of welded joint is essential in determining the material properties in separate joint zones, like the weld, HAZ and transition zone. Moreover, the results of such studies are an excellent base for verification of developed theoretical models.

Considering above facts, the main objective of this study are experimental studies on strain during tension of samples welded by laser-arc hybrid technology using GMAW method and Yb:YAG laser beam. Dantec Q-400 Istra multi-camera 3D correlation system is used to measure the distribution of strains during performed tests made on the base material and welded joint. Presented results include tension diagrams as well as a comparison of strain fields measured for the entire tension cycle.

Experimental set-up, hybrid welding. Laser beam emitted by D70 Trumpf laser head with maximum power up to 12 kW is used with electric arc in GMAW method (Figure 1). Laser head is equipped with collimator lens having a focal length *fc* = = 200 mm, and a focusing lens with a focal length *f* = = 400 mm. The diameter of the beam is set by chang-

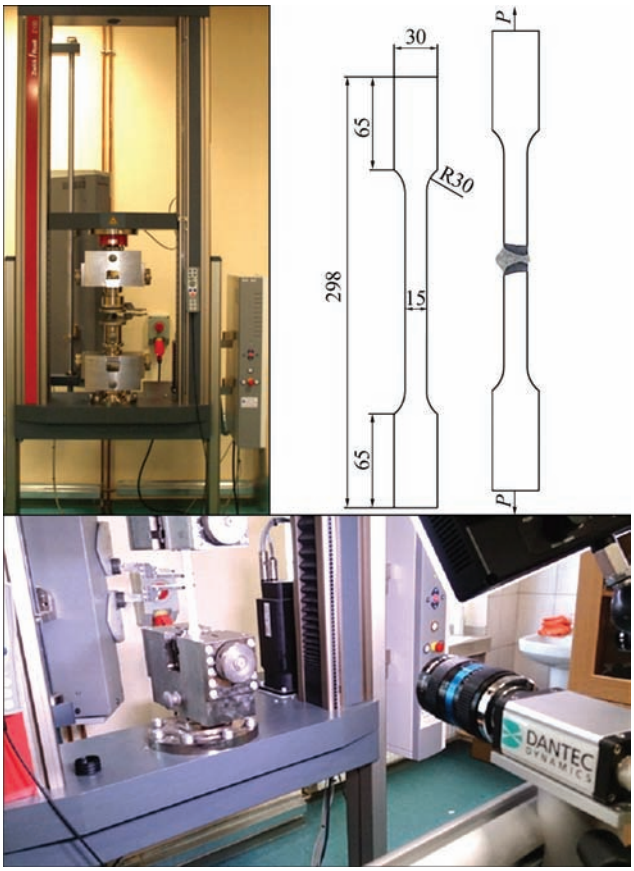

Figure 2. Tension test: universal strength machine Zwick&Roel Z100, dimension of samples used in the test, Q-400 ISTRA multi-camera 3D

ing the optical fiber supplying the laser beam to the head. Optical fiber is used in the research having a diameter 0.4mm. For used optical system double magnification is achieved giving laser focus diameter *d* = = 0.8 mm. Butt welding is performed for sheets made of S355 steel. Welding process proceed without a gap in the shielding gas 82 % Ar + 18 % CO_2, the gas flow is 18 l/min, wire speed 6m/min and welding speed set

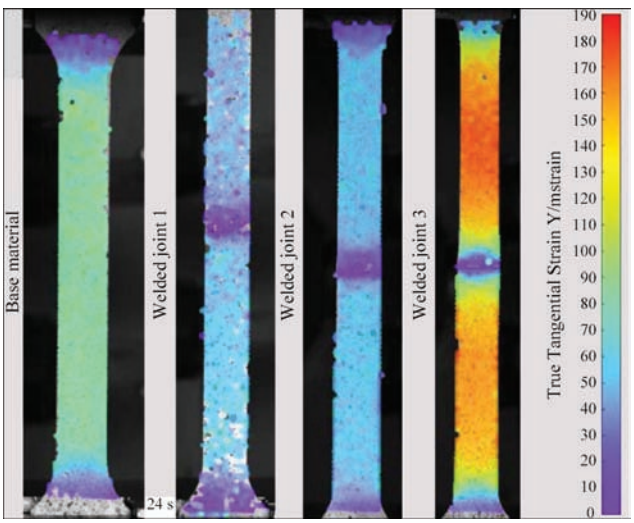

Figure 3. Strain fields in tensed base material and welded joint (*t* = 24 s)

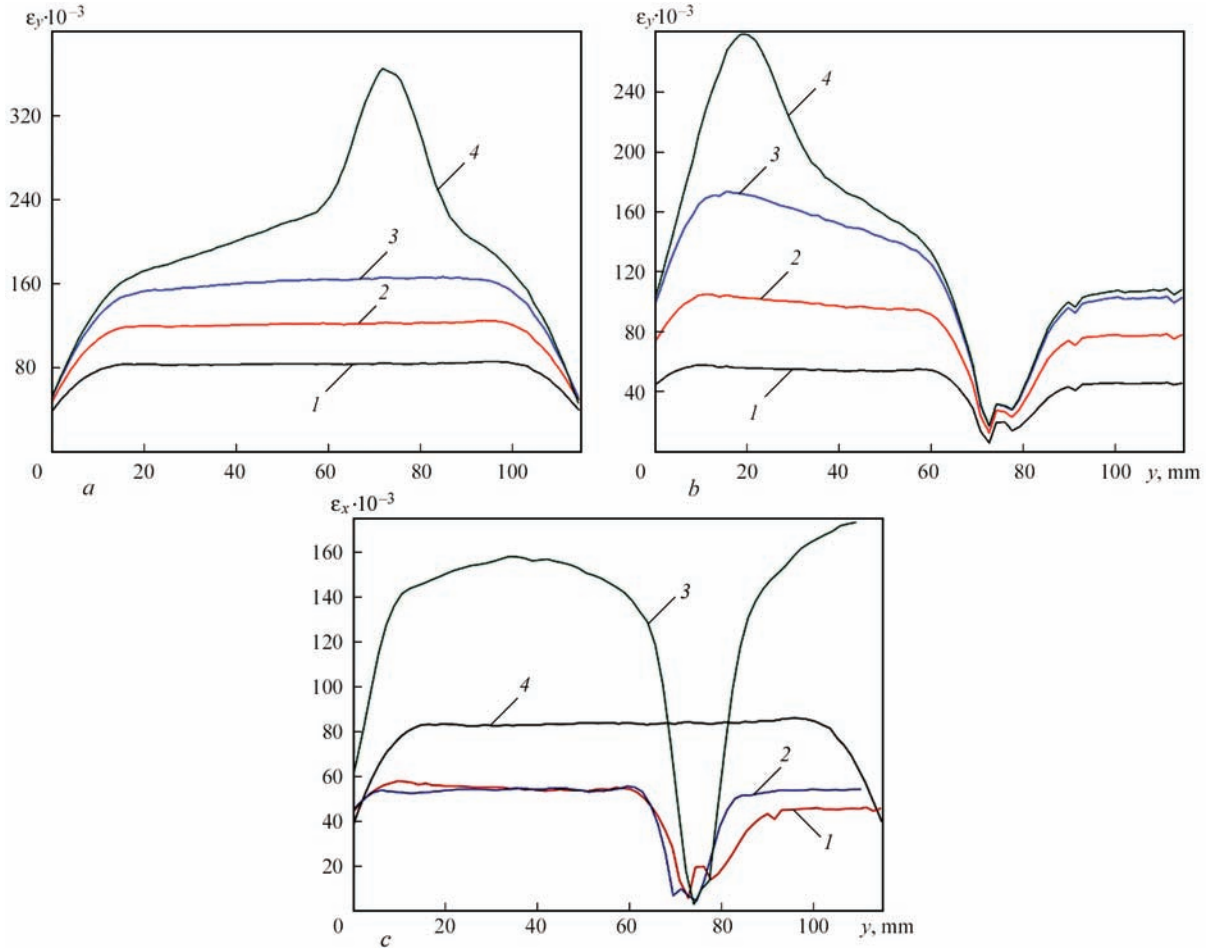

Figure 4. Distribution of strain ε_y in the central axis y of sample for different times of tension: *a* — the base material; *b* — welded joint; *c* — comparison for time t = 24 s (for a, b: 1 — 24s, 2 — 28, 3 — 32, 4 — 39; for c: 1–3 — welded joint 1–3; 4 — base material)

to v = 1 m/min. The distance between heat sources d = 2 mm. Laser beam is the leading heat source in the tandem.

Samples are welded in the system with leading laser beam in the tandem as well as in inversed system with leading arc. Laser beam power is set to Q = = 3 kW, arc voltage U = 19 V and current I = 190A in the welding experiment.

Strain measurement system. Samples for the tension test were made from welded joints according to norm PN-EN ISO 6892-1. Universal strength machine Zwick&Roel Z100 is used with extensometer Multisens in all performed tension tests. The accuracy of the strength machine is up to 0,1N in force and 1μm in displacement. Universal strength machine cooperates with Dantec Q-400 Istra multi-camera 3D correlation system [4–6]. Measurement system is composed of optical cameras used to record strains or deformations. The Timing Box is an interface between the control computer and the sensors for synchronization and analog recording of data, and to power-up cameras and PC computer with a number of network cards, allowing for the introduction of signals from cameras and different sources, transmitted via ethernet and installed dedicated Istra4D software.

In the experiment the system of three cameras was used. Cameras are mounted on the beam which is supported by two fully adjustable tripods. Optical cameras used to record strains and derormations are equipped with 50 mm, mod: 670 mm lenses and have maximum resolution 4.19 Megapixels, 29 Hz each. This allowed determining the full size of analyzed sample in the working area of universal testing machine. Strain fields are measured for the entire tension cycle. Trigger mechanism is created in Istra4D software for the measurement. Pictures are made for every time increment Δt = 0.4 s.

Results and discussion, strain distributions. Figure 3 presents comparison of strain fields in tensed base material and welded joint at the various measurement steps in elasto-plastic range as well as before the rupture-during the formation of the neck. It can be observed that the weld and HAZ has a significantly lower strain compared to the base material.

Distribution of strain εy along the length of tensed sample (55 mm in both direction from the center point

of the sample) is illustrated in Figure 4. Strain distribution is shown in the central axis y for the base material and welded joint at different times. Visible decrease of strain is present in the joint where HAZ is present. The slight increase of strain in the weld can be because of the inaccurate selection of an additional material in GMAW method.

The comparison of strain ε_y at time t = 24 s is presented in Figure 4, *c*. It can be observed that for the base material higher values of strain ε_y are present in comparison to welded joint.

Conclusions

The use of multi-camera 3D correlation system allowed the analysis of strain and deformation for the selected material points, lines or plane throughout the measuring sample. Use of the system allowed the analysis of deformation and strain distributions in the weld and heat affected zone during tension test. It can be observed that lower strains occur in heat affected zone in comparison to the base material which in reference to pictures of microstructure confirm partial hardening of this zone. Visible increase of strain εy in the weld may be due to the inaccurate selection of an additional material in GMAW method. Obtained results allowed for a thorough analysis of mechanical properties separate zones of the joint and do not limit the tensile test to determine the global strength and plastic properties of welded material. Obtained experimental results may be very helpful in verifying mathematical and numerical models of thermomechanical phenomena occurring in welding processes.

1. Patorski, K. (2005) *Interferometria laserowa*. Oficyna Wydawnicza Politechniki Warszawskiej, 214–261.
2. Herbst, C., Splitthof, K. *Basic of 3D Digital Image Correlation*. Ulm, Dantec Dynamics GmbH.
3. Chu, T.C., Ranson, W.F., Sutton, M.A, Peters, W.H. (1985) Application of digital-image-correlation techniques to experimental mechanics. *Experimental Mechanics*, 25(**3**), 232–244.
4. Gower, M.R., Shaw, R.M. (2010) Towards a planar cruciform specimen for biaxial characterization of polymer matrix composites. *Applied Mechanics and Materials*, **24–25**, 115–120.
5. Lord, J.D. (2009) *Digital Image Correlation (DIC), Modern stress and strain analysis. A state of the art guide to measurement techniques*. BSSM Technical Editors: J. Eaton Evans, J.M. Dulie-Barton, R.L. Burguete, 14–15.
6. Palanca, M., Cristofolini, L. *Validation and Optimalization of the parameters of Acquision and Processing For Analysis Through Digital Image Correlation*. University of Bologna.

Received 10.11.2017

doi.org/10.15407/tpwj2017.12.03

NEW POSSIBILITIES OF ADDITIVE MANUFACTURING USING XBEAM 3D METAL PRINTING TECHNOLOGY (Review)*

D.V. KOVALCHUK, V.I. MELNIK, I.V. MELNIK and **B.A. TUGAJ**
PJSC SPA «Chervona Hvilya»
15 Kazimir Malevich Str., 03150, Kiev, Ukraine. E-mail: dv_kovalchuk@yahoo.com

New technology called xBeam 3D Metal Printing was developed by PJSC SPA «Chervona Hvilya» to solve the most important engineering and economic problems of the currently available methods of additive manufacturing. It is based on application of shaped electron beam as the heat source and of wire as consumable material. The key element of the new engineering solution is a special low-voltage gas-discharge electron gun, with a guide built-in along its axis for consumable wire feeding. A unique hollow conical electron beam generated by such a gun, creates exceptional physical conditions for melting of consumable and its layer-by-layer deposition that not only provides the capabilities of precisely controlled and repeatable manufacturing of products, but also opens up the possibilities for development of new technologies and materials. At present xBeam 3D Metal Printing technology has successfully passed laboratory and practical trials in an experimental 3D-printer. 16 Ref., 13 Figures.

Keywords: *electron beam, gas-discharge electron beam guns, additive manufacturing of metals, 3D metal printing*

Over the last decade additive manufacturing has become one of the most important directions of development of world industry. Additive technologies open up the possibilities of rapid and accurate manufacturing of products by the customer individual requirements, which is a long-standing dream of any manufacturer. Owing to this unique capability, additive manufacturing is even called the third industrial revolution, alongside robotization and information technologies [1–3].

Additive manufacturing is defined as a process of product manufacturing according to a 3D model by layer-by-layer joining of materials using CAD/CAM. Additive manufacturing technologies are also called industrial 3D printing, and equipment for their realization — 3D-printers [4–6].

Particularly important is additive manufacturing of products from metals, as metals still are the main industrial structural material [7].

A variety of additive manufacturing technologies have been developed so far, differing by:

- consumable: powder, wire or powder in a mixture with binder;
- heat source: laser, electron beam, plasma, electric arc, etc;
- method of layer forming: selective melting (sintering) of the prepared powder layer (powder bed); direct deposition of powder or wire on the previous layer (direct energy deposition) or injection molding (binder jetting) [4, 5, 8].

Despite continuous research and numerous experiments, however, additive manufacturing technologies, developed so far, still have a number of drawbacks, restraining their extensive implementation in industry. The main shortcomings of additive technologies developed to date are as follows [9, 10]:

- sophisticated and expensive equipment;
- expensive initial materials;
- limited dimensions of manufactured 3D products and low efficiency (for technologies with application of powder as initial material);
- thick walls and rough surface of manufactured 3D products (for technologies with application of wire as initial material);
- residual porosity, non-uniform structure, residual stresses and strains;
- need for additional operations;
- complex control requiring highly skilled staff.

All that eventually leads to high product cost that markedly restrains the really wide acceptance of additive technologies in the world industrial production [11].

Specialists of PJSC SPA «Chervona Hvilya» developed a new method of manufacturing 3D objects and a device for its implementation [12], in which the product is formed by layer-by-layer deposition of consumable on a base. The consumable is fed into the

*By materials of a report made at VIII International Conference on «Beam Technologies in Welding and Materials Processing», September 10–16, 2017, Odessa.

© D.V. KOVALCHUK, V.I. MELNIK, I.V. MELNIK and B.A. TUGAJ, 2017

deposition zone, moved along the set trajectory, melted there by the electron beam and then it solidifies as it leaves the heating zone, forming the deposited material layer. The heat source in the above method and device is a gas-discharge electron beam gun with an annular cathode, directly generating the electron beam in the form of a hollow inverted cone.

The new technology called xBeam 3D Metal Printing, according to the generally accepted classification of different types of additive technologies, relates to direct energy deposition processes, where the focused thermal energy is used to melt materials at their deposition [4, 5].

In the opinion of both the developers and a number of experts in the field of additive manufacturing, xBeam 3D Metal Printing technology is capable of solving many engineering and technological problems of currently available additive technologies: primarily, eliminate the contradiction between the manufacturing accuracy and high productivity, and thus ensure a cardinal reduction of the cost of manufacturing 3D metal products.

Development of the new method is based on a unique ability of gas-discharge electron beam guns to generate shaped electron beams by direct emission from the cathode without application of additional deflecting and focusing devices [13]. Other characteristic capabilities of gas-discharge electron beam guns are also important for realization of the above technology and achievement of positive technological and economic effects. These features include the ability to operate stably in a broad range of residual pressures in the working chamber (10^{-2}–10 Pa), also at partial pressure of various gases, ability to generate and form the electron beam at relatively low accelerating voltage (from 5 kV), simple and compact design, convenient maintenance, long cathode life and flexible control of technological parameters.

The main distinctive features of the method and device underlying xBeam 3D Metal Printing technology are as follows:

- electron beam in the form of a hollow inverted cone, generated by a special gas-discharge electron beam gun, is used to form the melt pool on the substrate and to melt the consumable;
- consumable in the form of wire is fed through the guide precisely into the center of the melt pool on the substrate, coaxially with the above-mentioned conical electron beam;
- above-mentioned special gas-discharge electron beam gun and guide for feeding the consumable are combined into one common process module (Figure 1).

The above configuration of the electron beam, relative position of this beam and the fed consumable

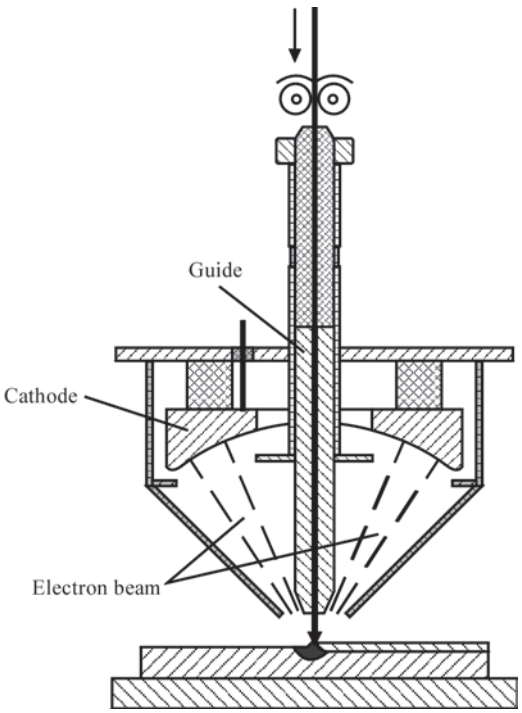

Figure 1. Schematic of a device for realization of xBeam 3D Metal Printing technology

with respect to the substrate create several critically important physical and metallurgical conditions for deposition of molten material and formation of the deposited bead. This results in controllable formation of the next layer with certain geometrical parameters and required structure of the deposited material. The following technological features of xBeam 3D Metal Printing should be noted first of all.

Round shape of the melt pool and vertical feed of the consumable precisely into the melt pool center (Figure 2) ensure absence of shaded areas on the substrate (preventing porosity and lacks-of-fusion in the deposited layers), possibility of forming a bead of a width only slightly exceeding the consumable wire diameter (that allows manufacturing products with thin and precise walls), overall high efficiency of the process due to effective use of the total power applied to the deposition zone.

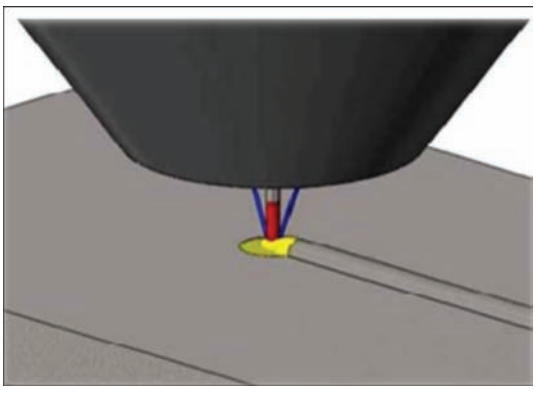

Figure 2. Schematic of the deposition process

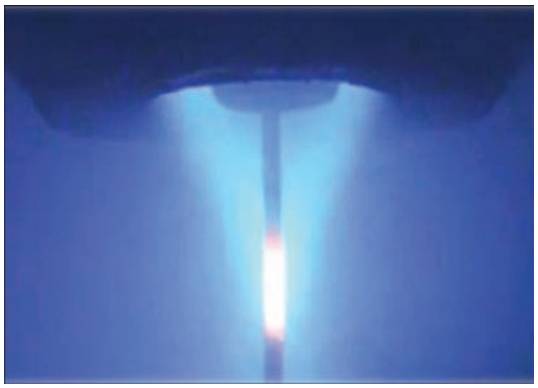

Figure 3. Impact of a hollow conical electron beam on consumable wire

Such an axisymmetric configuration of heat flows and mass transfer greatly simplifies mathematical modeling of the process that is very important for improvement of technological operations control to obtain the specified material properties [14].

The consumable is completely enclosed by precisely and flexibly controlled energy flow (Figure 3) that ensures its absolutely axisymmetric and uniform preheating and controlled melting. It is important to emphasize that the hollow beam configuration produced without scanning application, provides a really constantly uniform heating of both the wire and the substrate. Moreover, this property also opens up interesting possibilities in terms of technology, for instance use of complex consumable variants, such as flux-cored wire or bundle of several wires from different materials.

Continuous stationary mass transfer of liquid metal from the tip of melted consumable wire to the substrate is reliably contained by surface tension forces (Figure 4). As soon as liquid metal formed at the tip of fed wire touches liquid metal in the pool on the substrate, a bridge immediately forms between the wire tip and the substrate, which is contained by surface tension forces and along which the liquid metal smoothly and evenly flows onto the substrate, its speed being also influenced by the force of universal gravitation. The liquid metal, which has reached the substrate, immediately spreads within the boundaries of the melt pool existing at this moment of time, which is defined by the boundaries of the zone of electron beam impact on the substrate, due to complete adhesion between homogeneous liquids. As soon as liquid metal has reached solid metal on the substrate, it immediately solidifies. This is the way for realization of a reliable and at the same time flexible mechanism of forming a deposited bead of specified width and wall thickness of the manufactured 3D product, respectively.

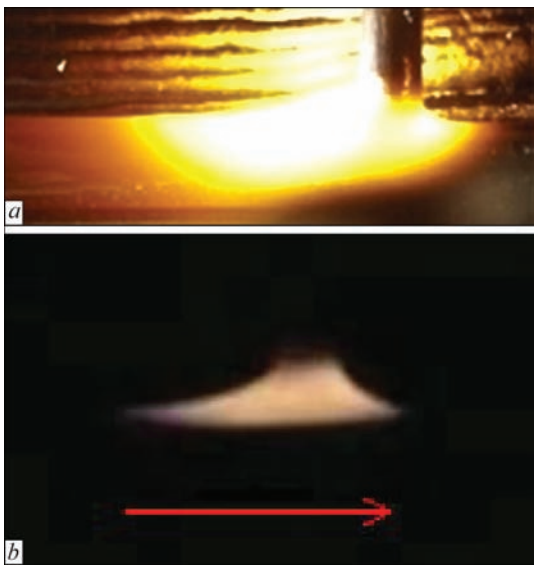

Figure 4. Liquid metal spreading from wire tip over the substrate: *a* — direct filming; *b* — filming through dark glass

It should be noted separately that the above property of continuous mass transfer of liquid metal from the wire tip to the substrate ensures the feasibility of xBeam 3D Metal Printing technology under the conditions of zero gravity, as the surface tension forces act there as they do on the Earth. The need for additive manufacturing of metal parts under zero gravity conditions on board the space vehicles, as well as in the missions to explore the Moon and Mars, is constantly emphasized in the plans of the respective organizations and companies, such as NASA, ESA, SpaceX and others [15, 16].

An extremely important property of xBeam 3D Metal Printing technology is significantly lower concentration of power of the heat source — the electron beam, generated by low-voltage gas-discharge electron beam gun, compared to heat sources of all the other currently known processes of additive manufacturing of metals. Developers of 3D-printers for metal usually apply devices (thermoionic electron beam guns, lasers, plasmatrons) developed for realization of welding processes, where the minimum possible focus (as a rule from tens up to hundreds of microns) and high power concentration (up to 10^5–10^7 kW/mm^2) are important process parameters. In additive manufacturing excessive power concentration can lead to a too deep penetration of the previous layers, right up to formation of defects in the product. Therefore, highly concentrated power has to be distributed over the surface by high-frequency scanning that, firstly, is a complex engineering task, and, secondly, violates the continuity of the process of deposited layer formation.

Special gas-discharge electron beam gun developed for implementation of xBeam 3D Metal Printing technology generates the electron beam at low accelerating voltage of up to 20 kV that at up to 20 kW power level and minimum focus of about 1.5 mm

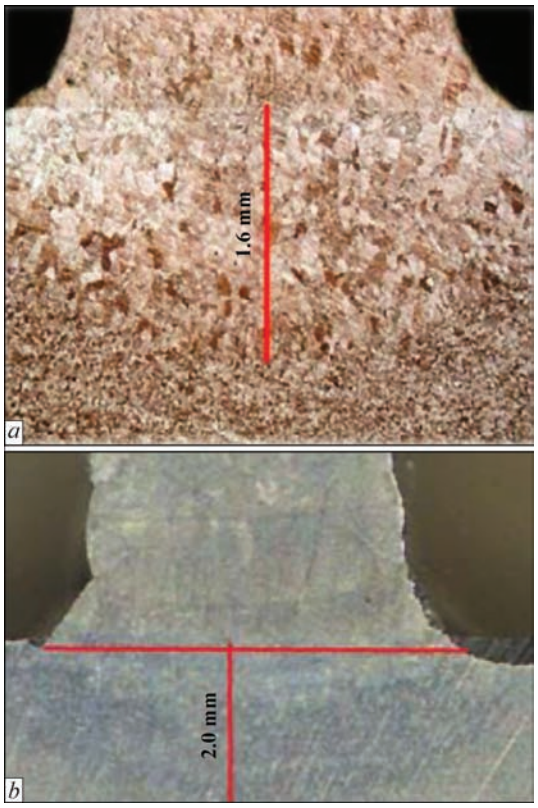

Figure 5. Macrosection of HAZ metal at wire deposition: *a* — 1.6 mm VT1-0 titanium wire on VT1-0 titanium plate; *b* — 3 mm Ti–6Al–4V titanium alloy wire on Ti–6Al–4V alloy plate

diameter provides a very soft and smooth heating of the processed surfaces without scanning application. Power concentration in electron beam focus does not exceed 10^3 kW/cm^2.

Impact of such a beam on the surface allows forming a quite shallow melt pool on it, sufficient only for creation of the conditions for spreading of entering liquid metal within the liquid phase on the surface, and having a minimum impact on substrate material.

Maintaining a shallow melt pool on the substrate during deposition (Figure 5) provides a higher deposition rate and rapid solidification of molten substrate material and deposited material, thus resulting in a better structure of the produced metal.

A smaller amount of material, being in the liquid phase per a unit of time, essentially reduces alloying element losses for evaporation that is particularly important for many alloys of titanium, niobium and other refractory metals. So, investigations of the change of chemical composition of titanium alloy Ti–6Al–4V during deposition by xBeam 3D Metal Printing technology showed a significant lowering of aluminium content from 5.91 % in the initial wire to 5.72–5.79 % (depending on process parameters) in the deposited material.

Lower power concentration on the deposition surface essentially reduces temperature gradients on the substrate and in the earlier deposited layers this provides lowering of residual stresses and strains.

Figure 6. Sample produced using wire as deposition substrate: *a* — side view; *b* — top view; *c* — bottom view

In order to demonstrate the positive effect from application of low-voltage electron beam, an experiment was conducted, in which wire was used as a substrate instead of the traditional thick plate, the wire ends being fastened by clamps. 3 mm wire from titanium alloy Ti–6Al–4V was used as the deposition material, and 3.2 mm wire from VT1-00 titanium was the substrate.

Set power of electron beam gun was 3 kW at accelerating voltage of 15 kV. The wire was fed at the rate of 14 mm/s, the substrate was also moved with the speed of 14 mm/s. The substrate was not preheated. The experiment resulted in building an even wall (Figure 6), corresponding by the main parameters (wall width and height, layer thickness) to a similar wall, deposited on a massive substrate. Here, residual buckling (distortion) of the substrate was completely absent, that is practically inevitable at application of a massive plate [14].

This feature can be quite effectively used in the case of building a product, where the base plate is not its part and should be removed completely by machining.

An important feature of xBeam 3D Metal Printing technology is a small number of basic process parameters and simplicity of their control that is extremely important for guaranteeing the repeatability and improvement of overall production efficiency. The main parameters of the process are as follows:

- electron beam gun power;
- size of gap *Z* between wire outlet and substrate (Figure 7);
- consumable wire feed rate;

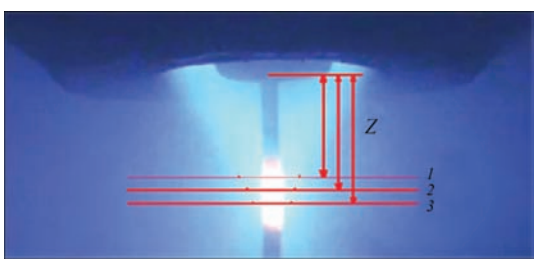

Figure 7. Gap *Z* between wire outlet and substrate

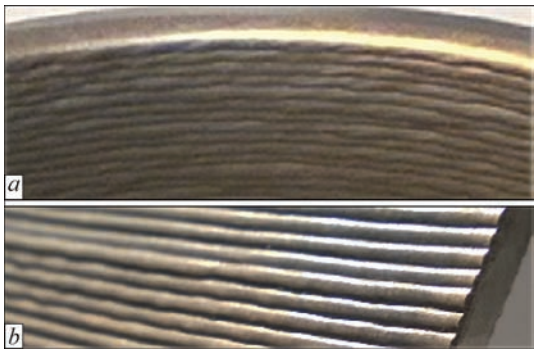

Figure 8. Walls formed from 2 mm wire: *a* — stainless steel 304L, 0.6 mm layer thickness; *b* — Ti–6Al–4V titanium alloy, 1.2 mm layer thickness

● linear speed of displacement of the substrate (deposition zone).

Note that wire of one diameter is used in the process.

The key parameter determining the main characteristics of the process of 3D product forming is exactly gap *Z* between the wire outlet and the substrate.

Size of gap *Z* determines electron beam power distribution between consumable wire and substrate, as well as the width of the zone of electron beam impact on the substrate (i.e. width of melt pool on the substrate), practically corresponding to that of the deposited bead. Thus, at constant power of electron beam, maintaining a stable size of gap *Z* ensures stable deposition rate, i.e. constant efficiency of deposition process.

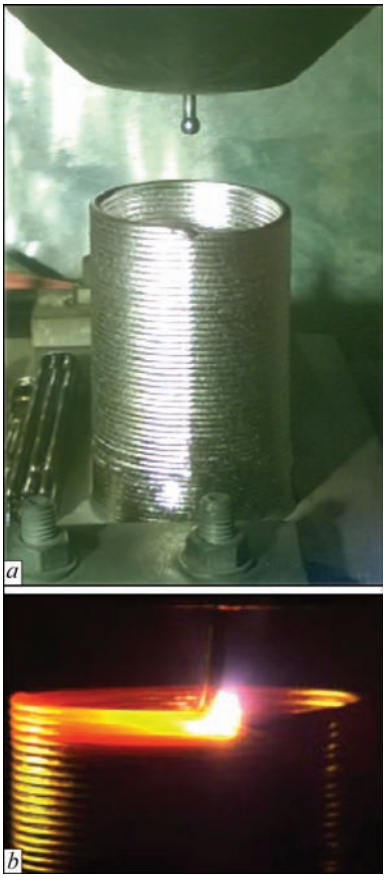

Figure 9. Sleeve from Ti-Grade 4 titanium (*a*), made by xBeam 3D Metal Printing technology (*b*) with 3 mm wire deposited in 50 layers at about 2.5 kg/h rate

An important advantage of the technology is the fact that stability of this key parameter of the process is ensured by simple observance of constant geometrical configuration of equipment components that is easily implemented by mechanical means and is also readily controlled.

Then, given the constant electron beam power and gap *Z*, i.e. at constant deposition rate and width of produced bead deposit, the height of deposited layer can be varied by changing linear speed of substrate displacement, as here the same quantity of entering liquid metal will be distributed over another area in direct proportion to the change of linear speed of substrate displacement.

Figure 8 shows walls with different parameters of deposited layers, formed from wire of the same diameter.

Thus, control of just several simple parameters of equipment provides flexible control of 3D product forming and guarantees repeatability of the main parameters of deposition of each layer (Figure 9).

At determination of the full set of controlled process parameters, the following can be also taken into account and controlled, accordingly: vacuum parameters, type of working gas in gas-discharge electron beam gun, temperature of deposition substrate, ratio of accelerating voltage and beam current at the same power.

An essential factor for choosing the right strategy of 3D product forming is selection of consumable wire diameter. xBeam 3D Metal Printing technology was initially oriented mainly to application of standard commercial wire of 1 to 3 mm diameter. This is an important argument in favour of improvement of cost effectiveness of the technology, as standard wire is always less expensive than the specially ordered one. More over, the wire price decreases considerably with increase of its diameter. Here, it is obvious that thin walls with less roughness can be more readily formed with smaller diameter wire.

Selection of optimum diameter of consumable wire becomes particularly important in manufacturing products with thick walls, exceeding the limit width of one bead deposit. In this case, the strategy of deposition of several parallel beads with a certain overlap between the adjacent passes is applied, as shown in Figure 10.

Figure 11 shows the macrostructure of a thick wall formed in several parallel passes.

One of the serious technological problems of currently available processes of additive manufacturing

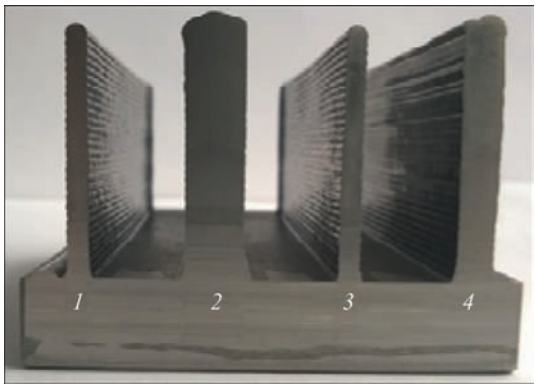

Figure 10. Walls of different thickness formed using xBeam 3D Metal Printing technology with 2 mm wire from titanium alloy Ti–6Al–4V at about 1.1. kg/h deposition rate: walls *1* and *3* in one pass, 3.1–3.3 mm thickness; *2* — in three passes; 10.0–10.3 mm thickness; *4* — in two passes, 6.0–6.2 mm thickness

of metals is formation of a columnar structure with upward growth, when the columnar grains grow through all the deposited layers. Such a structure is highly undesirable, as it leads to non-uniformity of properties in different directions. Owing to flexible possibilities of power distribution control and dynamic deposition process, providing quite high rates of solidification and subsequent cooling, xBeam 3D Metal Printing technology demonstrated the ability to prevent formation of a columnar structure in 3D metal products.

Figure 12 shows the macrostructure of a sample of titanium alloy Ti–6Al–4V, made from 2 mm wire with the deposition rate of about 0.9 kg/h. A structure of cast type was produced with grains close to equiaxed ones in their shape. Here, the grains grow through the adjacent deposited layers (not more than two), that confirms the absence of any interlayer peculiarities, segregations or defects. Investigations are carried on to determine mechanical properties, as well as the

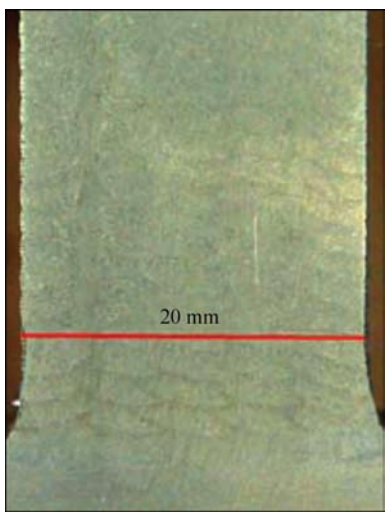

Figure 11. Macrostructure of a thick wall formed in five parallel passes. Titanium alloy Ti–6Al–4V, 3 mm wire, about 2 kg/h deposition rate

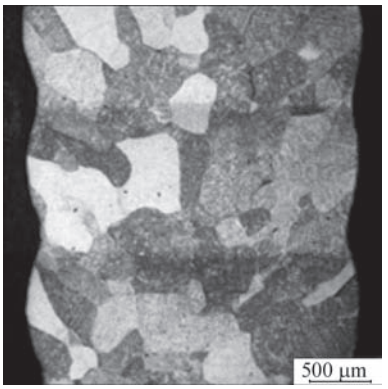

Figure 12. Macrostructure of a sample of titanium alloy Ti–6Al–4V

influence of process parameters on the structure and properties of materials, produced by layer-by-layer deposition by xBeam 3D Metal Printing technology.

During trial manufacturing of real industrial parts from titanium alloys, direct and associated operating costs, as well as the yield were assessed in manufacturing products by xBeam 3D Metal Printing technology. Received estimates showed operating cost for titanium alloys on the level of 40 USD per 1 kg of finished product, taking into account the final machining to bring the part to its finished shape. This corresponds to the value of not less 0.01 USD per 1 cm^3 of deposited material, being the lowest index among all of the currently available processes of additive manufacturing of metals.

A pilot unit xBeam-01 was developed and manufactured for realization of xBeam 3D Metal Printing technology, studying its capabilities and optimizing the basic process techniques (Figure 13). The unit features a simple and compact design: 10 m^2 of useful area is enough for its operation, i.e. it can be installed even in a university laboratory. Consumable can be loaded in without breaking the vacuum in the working chamber that is very convenient for research

Figure 13. xBeam-01 unit

performance. Features of operation of gas-discharge electron beam gun allow conducting the process in low vacuum — within 10^{-2}–10^{-1} mbar, so that the unit is fitted with one mechanical backing pump. Application of low accelerating voltage in the electron gun (10–15 kV) results in improvement of personnel safety in terms of the impact of X-ray radiation from the chamber.

Specification of xBeam-01 unit is given below.

Useful size (L×W×H), mm	300×300×300
Positioning system	Three-axis, linear
Maximum power, kW	20
Limit accelerating voltage, kV	20
Maximum power consumption, kW	30
Limit vacuum, Pa	5.10^{-1}
Working vacuum, Pa	10–50
Possible kinds of consumables	Wire, rods, flux-cored wire of 1–3 mm dia.
Working gas (helium) flow rate, at 0.1 MPa, l/min	2.5
Recommended working space (W×L×H), mm	330×3000×2400
Total weight, kg, approximately	1500

During performance of experimental work in xBeam-01 unit deposition rate of 700 cm^3/h has been achieved so far that corresponds to more than 3 kg/h for titanium alloys. Here, the accuracy of 3D product manufacturing and surface roughness require subsequent finish machining of not more than 1 mm on each wall that is much better than for the currently available analogs. Electron beam gun rated power on the level of just about 7 kW was sufficient to achieve such efficiency. This allows anticipating achievement of not less than 2000 cm^3/h deposition rate at maximum rated power of the gun that corresponds to maximum values demonstrated so far in the market of additive technologies.

Development of CAM software is carried on, as well as testing of means of monitoring and analysis of process parameters and equipment.

Proceeding from pilot unit experimental operation and performed upgrades, PSJC SPA «Chervona Khylya» specialists are developing prototypes of serial units of laboratory and commercial grade.

New additive manufacturing electron beam technology xBeam 3D Metal Printing and 3D-printers of xBeam family promise to become reliable and efficient equipment for rapid and high-quality manufacturing of complex parts and for research work, owing to application of inexpensive standard commercial materials (wires) as consumables, minimum material losses at final machining, defectfree structure, simple and safe operation and reasonable price of equipment.

1. *A third industrial revolution*. The Economist, http://www.economist.com.node/21552901.
2. *Is 3D printing the next industrial revolution?* TechCrunch, https://techcrunch.com/2016/02/26/is-3d-printing-the-next-industrial-revolution/
3. (2013) *Additive manufacturing market outlook. Value chain-Market size-Key players-Business models*. Additive manufacturing. A game changer for the manufacturing industry? Strategy Consultants GmbH, Roland Berger, 19–24.
4. *ISO/ASTM 52900:2015 (ASTM F2792)*: Additive manufacturing. General principles. Terminology.
5. *Wohlers Report 2017. 3D printing and additive manufacturing: State of the industry annual worldwide progress report*. ISBN 978-0-9913332-3-3.
6. *What is additive manufacturing?* AdditiveManufacturing.com, http:// additivemanufacturing.com/basics/
7. Zaleski, A. (2015) Here's 3D printing needs more metal. *Fortune*, **11**.
8. *3D printing processes*: The free beginner's guide, http://3d-printingindustry.com/3d-printing-basics-free-beginners-guide/processes/
9. Chaplais, Ch. (2016) *7 challenges to a wider adoption of additive manufacturing in the industry. Manufacturing transformation*, http://www.apriso.com/blog/2016/07/7-challenges-to-a-wider-adoption-of-additive-manufacturing-in-the-industry-part-1/
10. Gao, W., Zhang, Y., Ramanujan, D. et al. (2015) The status, challenges, and future of additive manufacturing in engineering. *Computer-Aided Design*, **69**, 65–89.
11. Douglas, S.T., Stanley, W.G. (2014) *Costs and cost effectiveness of additive manufacturing*. NIST Special Publication 1176.
12. Kovalchuk, D.V., Melnyk, V.G., Melnyk, I.V., Tugaj, B.A. (2016) *Method of manufacturing of 3D objects and device for its realization*. Pat. 112682 Ukraine [in Ukrainian].
13. Kovalchuk, D., Melnyk, V., Melnyk, I., Tugai, B. (2016) Prospects of application of gas-discharge electron beam guns in additive manufacturing. *Electrotechnics and Electronics (E+E)*, **5–6**, 36–42.
14. Makhnenko, O.V., Milenin, A.S., Velikoivanenko, E.A. et al. (2017) Modelling of temperature fields and stress-strain state of small 3D sample in its layer-by-layer forming. *The Paton Welding J.*, **3**, 7–14.
15. Ghidini, T. (2013) *An overview of current AM activities at the European Space Agency*. 3D printing & additive manufacturing — Industrial applications. Global Summit 2013 (London, UK).
16. Clinton, R.G. Jr. (2017) NASA Marshall Space Flight Center Additive Manufacturing: Rocket engines and in space manufacturing. In: *Proc. of 2nd Int. Symp. on Additive Manufacturing* (February 8–9, 2017, Dresden, Germany).

Received 31.10.2017

doi.org/10.15407/tpwj2017.12.04

APPLICATION OF EXPLOSION WELDING FOR MANUFACTURE OF TRIMETALLIC TRANSITION PIECES OF CRYOMODULES OF LINEAR COLLIDER

A.G. BRYZGALIN[1], **E.D. PEKAR**[1], **P.S. SHLENSKY**[1], **G.D. SHIRKOV**[2], **Yu.A. BUDAGOV**[2] and **B.M. SABIROV**[2]

[1]E.O. Paton Electric Welding Institute of the NAS of Ukraine
11 Kazimir Malevich Str., 03150, Kiev, Ukraine. E-mail: office@paton.kiev.ua

[2]JINR
6 Joliot Curie Str., 141980, Dubna, RF. E-mail: post@jinr.ru

An original design of transition piece for joining cryomodules of linear collider was proposed, providing necessary strength, helium and vacuum tightness at relatively low cost. The modes of explosion welding of plane titanium–stainless steel–titanium workpieces, at which intermetallics in the joining zone are almost absent, were developed. The modes of electron beam fillet welding of niobium branch pipe with titanium of a transition disc were selected experimentally. The experimental samples of transition pieces were manufactured which successfully passed tests on thermocycling and helium tightness. 8 Ref., 11 Figures.

Keywords: *collider, explosion welding, helium tightness, transition piece, nuclear research*

The unique international project of the linear collider, being developed at the present time, has a great importance for fundamental research in the field of nuclear physics and power engineering [1]. Its peculiarity consists in the fact that accelerated particles will collide in vacuum space at the temperature, close to absolute zero. The length of the collider will be more than 50 thou m. It should consist of separate cryomodules of 1 m length, joined between each other by transition pieces.

The joined elements of the cryomodule are a niobium superconducting resonator, which should be welded-on by electron beam welding (EBW) to the niobium branch pipe and casing of stainless steel (type 316L) coaxially located with respect to the niobium resonator, welded-on to the disc of the transition piece manufactured of the same stainless steel. The vacuum niobium resonator is located inside the stainless steel casing, a liquid helium is filled under the casing (Figure 1). Thus, the transition piece should provide a vacuum and helium tightness. and serviceability of the unit under the conditions of high-frequency electromagnetic loads at cryogenic temperatures [2].

It is known that the most quality welded joints are produced in welding of homogeneous materials. Thus, the transition piece should provide producing welded joints of niobium with niobium and stainless steel with stainless steel, i.e. the transition piece should consist of at least two metals: niobium and stainless steel. The use of any methods of fusion welding, including EBW, for producing joints of niobium with stainless steel, is unacceptable for solving the specified problem in connection with the formation of intermetallics of type Nb_xFe_y, which do not allow providing the required tightness of the transition pieces.

We manufactured a transition piece by explosion welding-on of a niobium branch pipe directly to the disc of stainless steel. It was expected that much less intermetallics would be formed due to absence of high-temperature heating in explosion welding and they would not violate the tightness due to a large area

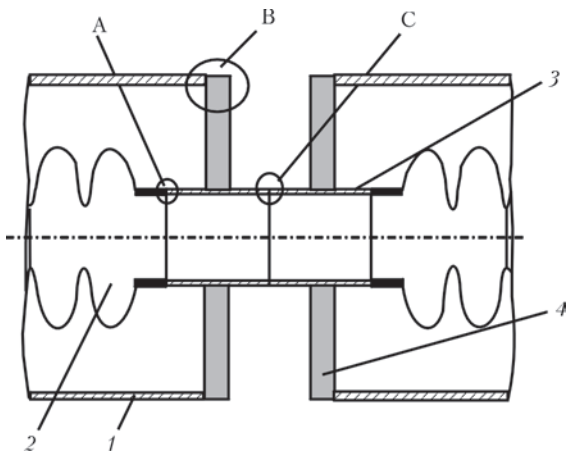

Figure 1. Scheme of cryomodules joining: *1* — casing of stainless steel; *2* — niobium resonator; *3* — niobium pipe; *4* — disc of stainless steel; A — joining of resonator with niobium pipe by EBW; B — joining of casing with the disc of transition piece by EBW or argon-arc welding; C — joining of niobium pipes of transition pieces by EBW

© A.G. BRYZGALIN, E.D. PEKAR, P.S. SHLENSKY, G.D. SHIRKOV, Yu.A. BUDAGOV and B.M. SABIROV, 2017

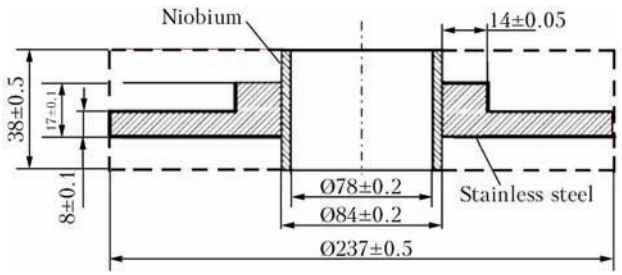

Figure 2. Scheme of manufacture of transition piece, using the explosion welding of niobium with stainless steel

of the joint [3]. Moreover, in order to preserve the integrity of the niobium pipe at the moment of explosion, the width of steel workpiece should be not less than the width of the niobium pipe. In Figure 2 the dotted line indicates the dimension of steel workpiece before the explosion.

To provide the required geometric dimensions of the transition piece, taking into account the inevitable deformations of niobium from explosion, it is necessary to use a niobium pipe with a smaller outer diameter and a larger wall thickness so that after explosion welding a transition piece with the necessary dimensions can be manufactured using machining. During machining a part of niobium and a significant part of stainless steel will make chips. Therefore, this method is not suitable for industrial application because of a high labor consumption, high cost and high consumption of scarce niobium. The helium tightness of the joint was not investigated.

The earlier carried out experiments showed, that in electron beam welding of niobium with titanium the intermetallics were not formed and the necessary tightness of joints was provided as to helium and vacuum. In this regard, the following variant of manufacturing the transition piece was proposed.

At first the disc of stainless steel is cladded with titanium on both sides applying explosion welding, then, after giving the necessary shape to trimetal (by straightening and turning to size), a hole is cut out for a niobium branch pipe. The branch pipe is inserted into the hole and welded-on to the titanium applying EBW (Figure 3). The possible formation of intermetallics in the joint of titanium with steel produced by explosion welding does not affect the transition piece

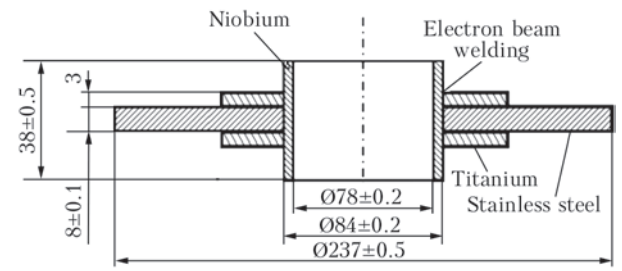

Figure 3. Design of transition piece, which provides absence of formation of niobium intermetallics during welding

serviceability, since helium can not enter the niobium pipe cavity through it.

The advantages of the proposed variant of manufacturing the transition piece:

- helium .tightness is provided by welding niobium with titanium, which have a good weldability;
- the hole in the flange is made according to the niobium pipe size, moreover, the branch pipe of the resonator can be welded-in instead of the pipe-transition piece;
- the possible formation of intermetallics in the joint area of steel with titanium during explosion welding does not affect the helium tightness;
- technologically, the explosion welding of plane specimens is much easier than welding of pipe billets and allows producing joints with the maximum possible stability of quality, which reduces the probability of rejection;
- after explosion welding, if necessary, the cheaper steel-titanium workpieces will be rejected;
- steel-titanium flange can be subjected to heat treatment to reduce residual stresses in a conventional (non-vacuum) furnace;
- the consumption of steel and niobium is reduced.

The titanium-steel joint is rather difficult to weld by explosion due to the fact that these metals form brittle chemical compounds during welding and subsequent heat treatment. It should be noted that titanium forms intermetallics with almost all metals except of niobium, tantalum and vanadium. In particular, during welding of titanium with steel the brittle intermetallic compounds Fe_2Ti and FeTi are formed. In case of formation of significant amount of intermetallics (in the form of solid interlayer), the joint strength is reduced to zero. The separate rare spot inclusions do not affect the static strength of the joint [4].

For the growth of intermetallic phase, the necessary condition is not only a high temperature, but also a certain time when high temperatures exist, i.e. a latent period. The explosion welding, being a very rapid process, provides a minimum time for staying the contact zone under the influence of high temperatures. This is the advantage of using explosion welding for creating the similar combinations of metals and alloys [5].

Experimentally, the modes for explosion welding of the titanium-steel-titanium trimetal were selected. Thickness of titanium was 3 mm and that of steel was 8 mm. The plates of 250×250 mm and 300×700 mm were welded. The straightening of plates after the first explosion and after manufacture of trimetal was carried out in industrial roll mills, at first in three-roll (the workpiece was given an arched shape) to eliminate local deformations, and then in nine-roll mills to

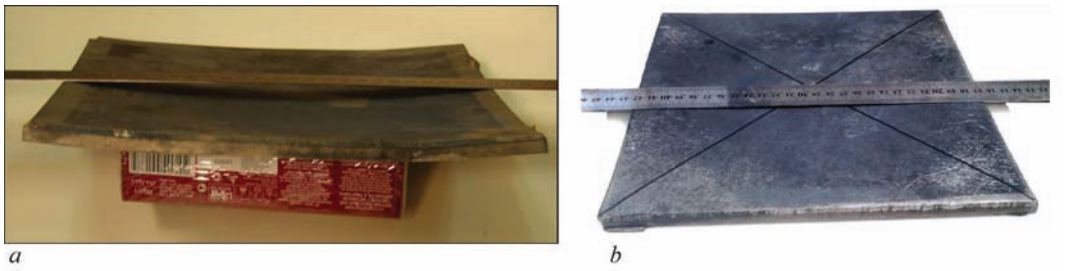

Figure 4. Appearance of workpiece produced by explosion welding: *a* — before straightening; *b* — after straightening

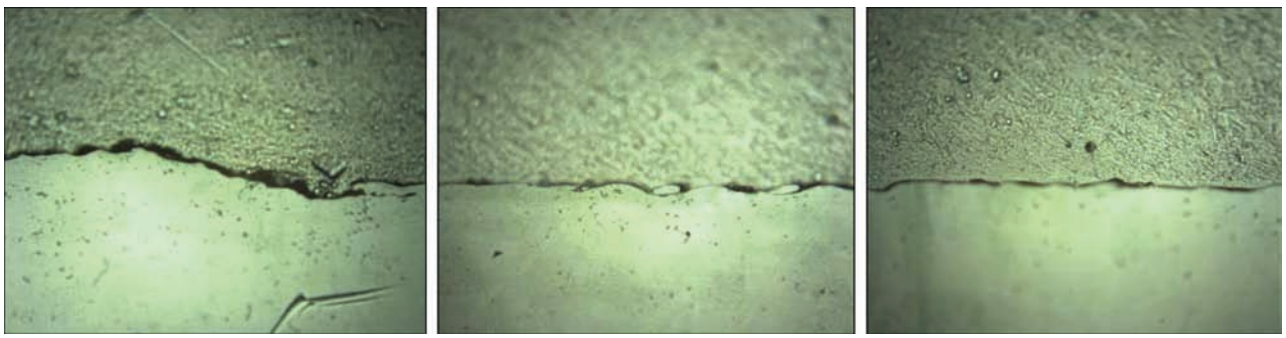

Figure 5. Microstructure (×400) of steel-titanium joint produced by explosion welding

make the plane.workpiece. The need in straightening is shown in Figure 4.

The discs of 237 mm diameter with a central hole for niobium branch pipe of 84 mm diameter were cut out of trimetallic workpieces. The maximum residual deflection of the disc was 0.5 mm.

In Figure 5 the photos of microsections with characteristic areas of the steel-titanium joint are given, produced in the selected welding modes. The waviness formation is almost absent, which evidences about the selection of the optimal mode for this case with the minimum power input, which reduces the number and size of the forming intermetallics.

On the microsection along the boundary of the joint, the elongated dark bands and also white spots of a small size can be occasionally, seen, which can be intermetallics.

To determine the nature of bands and spots, the investigations of microhardness were carried out applying Vickers method. The results of hardness measurements at a load of 100 g are shown in Figure 6.

The width of dark bands was of the order of 10 μm. Near the boundary of the joint the microhardness was measured by the dark bands. The hardness of the original titanium was 1300–1600 and that of the initial steel was 1700–1900 MPa. It is known that the hardness of intermetallics of type Fe_xTi_y is .above 9000 MPa. It is seen from Figure 6 that titanium and steel undergone a significant hardening as a result of collision during explosion welding, the titanium has its initial hardness already at a distance of 300 μm from the boundary, the steel is hardened to a greater depth. The achieved hardening can not affect the operating properties of the transition piece [6]. The absence of sharp hardness jumps near the boundary evidences that the dark bands are not intermetallics.

In the process of investigation it was established that there is a step on the boundary of the joint, which could have formed as a result of etching during the manufacture of a section or for other reasons. Apparently, the dark bands represent either contaminations accumulated along the step during grinding, or a shadow from the step, formed as a result of the section illumination by the microscope lamp.

Measurement of the microhardness of white spots and steel around them at a load of 10 g showed their equivalence and indicates that they are not intermetallics.

The quality of the titanium–steel joint produced by explosion welding was evaluated by standard test methods: on bending, on separation and shearing of layers [7].

Figure 7 shows the specimen after the bend test.

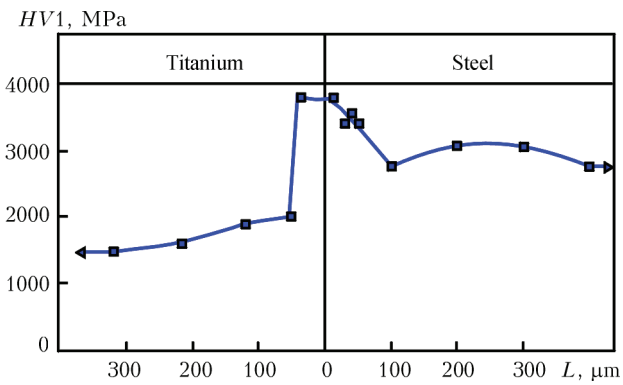

Figure 6. Microhardness at the boundary of steel-titanium explosion welding

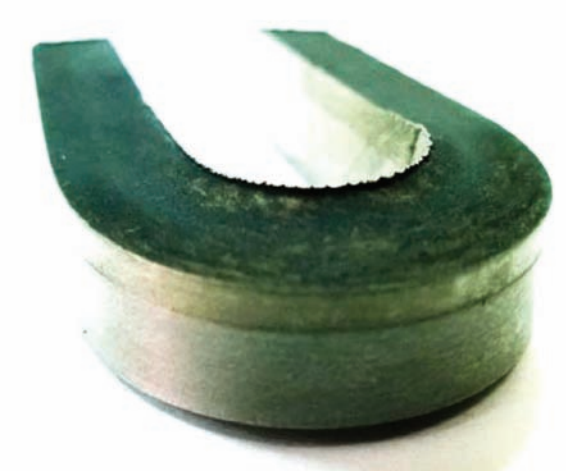

Figure 7. Specimen of steel-titanium bimetal after bending test

During bending at the angle of 180°, the specimen preserved its integrity, the delamination did not occur. This is a rather rigid type of tests, during low-quality welding the boundary of the joint of metals is destroyed.

Figure 8 shows the scheme of test for tear of bimetal layers and the general appearance of specimens.

The fracture of specimens occurred at the, steel-titanium interface, which is typical for this pair of metals [8]. The rupture strength amounted to 375 MPa. The tensile tests of sheet titanium in the initial state showed that the yield strength amounts to 390 MPa and that of tensile strength is 430 MPa. The strength of the joint is not too much inferior to the strength of the less strength metal among the those being joined.

The shear tests of layers (Figure 9) showed the strength at the level of 350 MPa. Such a high shear strength, which is comparable to the tear strength, is achieved due to the wavy boundary of the steel-titanium joint.

The service conditions of the transition piece do not imply the application of loads to it, leading to shear or tear of the layers, the strength of the joint can be considered satisfactory.

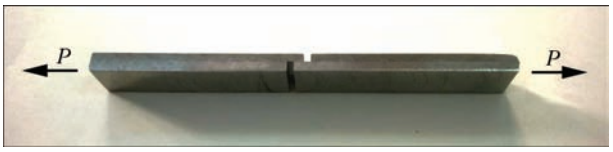

Figure 9. Scheme of test of specimen for shear strength of the layers

Thus, the carried out investigations allow stating that the developed mode of welding the trimetallic workpiece of the transition piece is close to optimal.

The cold working of metals and residual stresses in the produced trimetal can be removed by heat treatment. The safe heating for this composition is the heating of up to 600 °C. During heating above 700 °C, the intensive formation of intermetallics and carbides begins [4].

In case of welding titanium with stainless austenitic steels, the problem of need in heat treatment should be separately examined, as far as during heating and cooling the austenite can be transformed into martensite, which changes the properties of steel, including its magnetization, which reduces the efficiency of the collider.

The efficiency of applying heat treatment for improving mechanical properties of trimetal was investigated on specimens after heat treatment of workpiece at the mode of 600 °C, holding — 1 h, cooling in air. The tear strength of the layers was 325 MPa (375 MPa without heat treatment), the shear strength of layers was 345 MPa (350 MPa without heat treatment). The significant differences in the microstructure of metals in the joint zone as compared to the specimen without heat treatment, manufactured of the same trimetal workpiece, were not revealed. The Vickers microhardness at a load of 10 g amounted to: for steel — 2500 MPa (2600 MPa without heat treatment), for titanium — 2600 MPa (2150 MPa without heat treatment). On microsections at the joint boundary, a greater number of white spots was detected which have microhardness of 2300 MPa and are not intermetallics. They are, most likely, the areas of met-

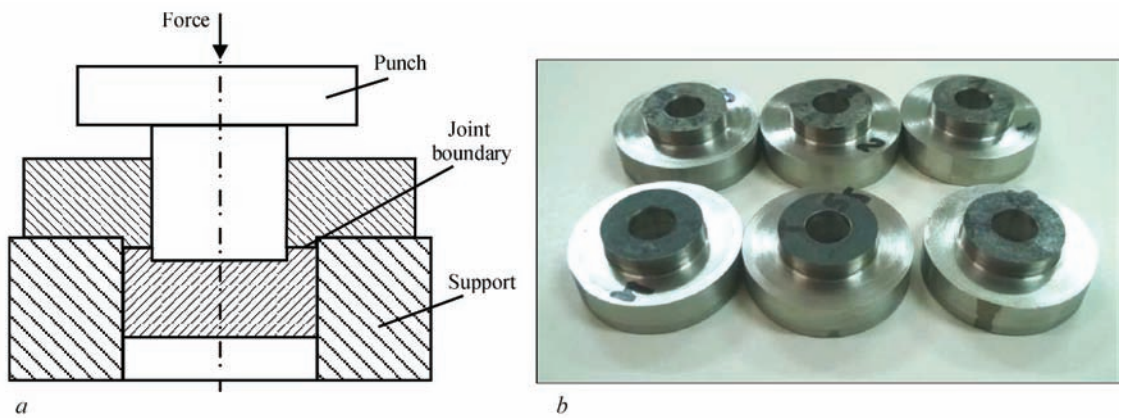

Figure 8. Scheme of tear test of bimetal layers (*a*) and general appearance of specimens (*b*)

al micro-overlaps, formed during explosion welding. The intermetallics in the investigated sections were not found. Thus, the heat treatment according to the mode mentioned above did not affect the properties of the trimetal required in the work. An increase in the annealing temperature is undesirable, as far as it can lead to appearance of intermetallics and a change in the properties of austenitic steel. Preliminarily, it can be concluded that it is not reasonable to perform heat treatment of trimetal billets, as it only increases the cost of the transition piece.

Selection of EBW modes. The use of high-purity niobium for manufacture of resonators demands for the performance of any thermal operations with it, including welding in vacuum. EBW is the most suitable for our case, since the process occurs in a chamber with a high degree of evacuation.

To perform EBW, the parts being welded should adjoin each other as close as possible. Since the niobium pipe has an initial ovality, along the circumference of adjoining the niobium branch pipe to the edge of the hole in the trimetallic disc, there are places with a larger gap not suitable for EBW. To eliminate this drawback, a device was manufactured, which fixes the branch pipe in the hole of the disc. The disc with the clamped branch pipe was inserted into the cartridge of the turning lathe, the roller was fixed instead of the cutter. By rolling the niobium branch pipe from the inside, its tight adjoining to the edges of the disc hole was achieved.

During manufacture of the experimental transition piece, the preliminary EBW mode was applied. The investigations of structure of the joint showed that the penetration depth of titanium was approximately 1 mm. According to statement of EBW experts, having a large experience in producing tight welds, including by helium, such penetration is rather sufficient to provide helium tightness. At the same time, the transition piece can be influenced by the loads generated from the excessive pressure inside the cryomodule due to the presence of vacuum on the outer side of the transition piece, as well as due to the possible heating of liquid helium from the elements of the cryomodule design during its filling with liquid helium and thermal conductivity of the transition piece, contacting the casing around the contour. In this connection, it seems rational to produce the weld as much strong as possible while, at the same time, preventing the full penetration of titanium and niobium by electron beam. On the model specimen the niobium branch pipe was welded-in to the titanium disc of 3 mm thickness using four EBW modes. Figure 10 shows the sections of the produced joints and the welded joint width is indicated.

The largest penetration was achieved at the modes 3 and 4. These modes will be used in manufacture of the subsequent transition pieces. The specific choice will depend on thickness of titanium, remaining after machining during manufacture of the disc of a trimetallic workpiece.

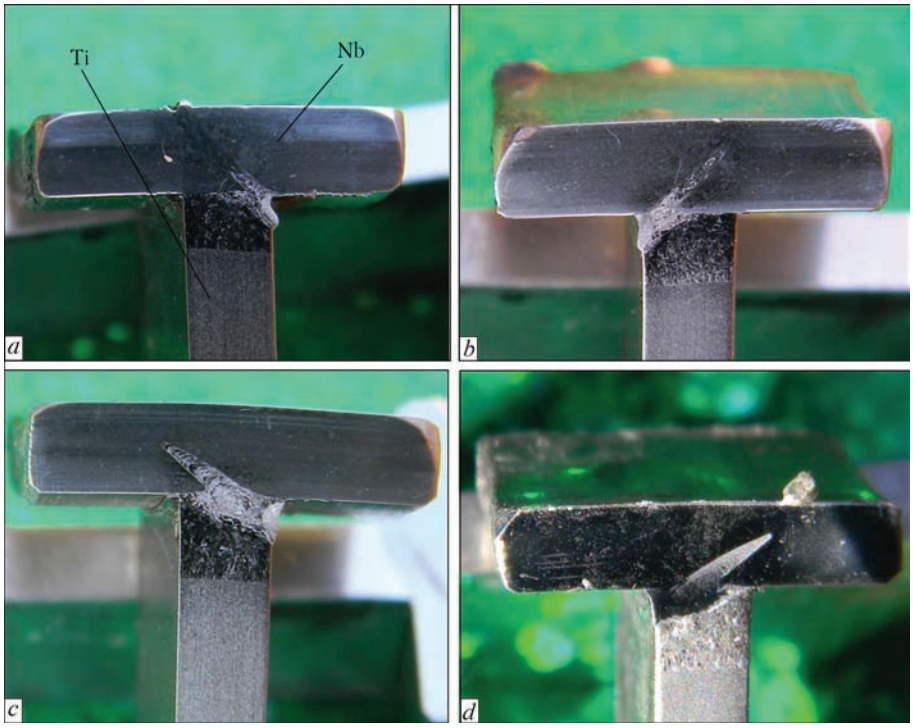

Figure 10. Sections of titanium–niobium joint produced by EBW: *a* — mode 1 (joint width is 1.5 mm); *b* — mode 2 (joint width is 1.9 mm); *c* — mode 3 (joint width is 2.75 mm); *d* — mode 4 (joint width is 2.1 mm)

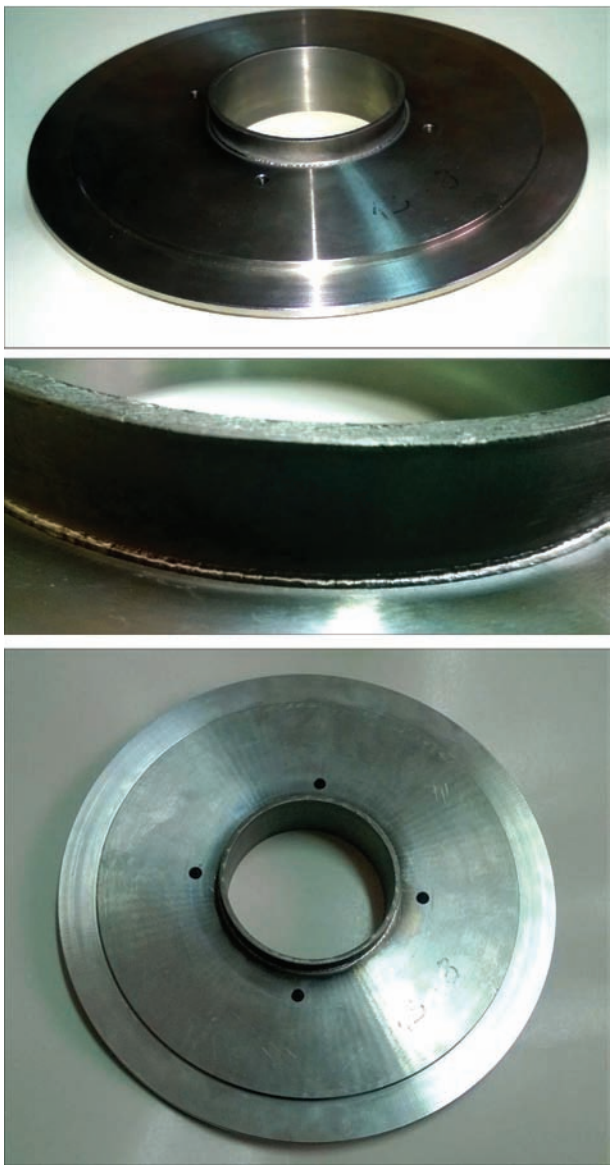

Figure 11. Appearance of manufactured transition piece

For today, two transition pieces were manufactured, one of which was subjected to heat treatment. Both transition pieces were tested for thermal cycling in liquid nitrogen and then in liquid helium. After each type of thermal cycling, the transition pieces were tested for helium tightness. In all the cases the positive results of tests were obtained.

Figure 11 shows the variants of appearance of the transition piece. The holes were made to carry out some investigations, the real transition piece will have no holes.

Conclusions

1. The design of transition piece, suitable for manufacture of cryomodule of a linear collider was developed which allows excluding welding-on of niobium to steel.

2. The technology of explosion welding the trimetallic workpiece for manufacture of transition piece was developed, providing the absence of intermetallics at the boundary of the steel-titanium joint.

3. The modes of EBW of niobium with titanium were selected, which, according to the preliminary evaluations, should meet the service requirements of the transition piece.

1. International Linear Collider. (2013) *Technical Design Report.* www.linearcollider.org/ILC/Publications/Technical-Design-Report.
2. Sabirov, B. (2010) Explosion welding: New design of the ILC cryomodule. *JINR NEWS*, **3**, 16–20.
3. Lysak, V.I., Kuzmin, S.V. (2005) *Explosion welding*. Moscow, Mashinostroenie [in Russian].
4. Gurevich, S.M. (1981) *Reference book on welding of nonferrous metals*. Kiev, Naukova Dumka [in Russian].
5. Ryabov, V.R., Dobrushin, L.D., Moon, J.G. (2003) *Welding of bimetal*. Ed. by Paton B.E. Kiev, PWI.
6. Petushkov, V.G., Fadeenko, Yu.I. (1995) *Explosion-thermal treatment of welded joints*. Ed. by Paton B.E. Welding and Surfacing Review; Vol. 8, Pt 2. London, Harwood acad. publ.
7. Petushkov, V.G., Simonov, V.F., Sedykh, V.S., Fadeenko, Yu.I. (1996) *Explosion welding criteria*. Ed. by Paton B.E. Ibid., Vol. 3, Pt 4. London, Harwood acad. publ.
8. Petushkov, V.G. (2009) *Explosion and its applications in metalworking*. New York, Nova Science Publ.

Received 27.11.2017

doi.org/10.15407/tpwj2017.12.05

ELECTROSLAG SURFACING OF END FACES WITH LARGE-SECTION ELECTRODE IN CURRENT-SUPPLYING MOULD

Yu.M. KUSKOV, V.G. SOLOVIOV and **V.A. ZHDANOV**
E.O. Paton Electric Welding Institute of the NAS of Ukraine
11 Kazimir Malevich Str., 03150, Kiev, Ukraine. E-mail: office@paton.kiev.ua

It is proposed to perform electroslag surfacing of end faces with application of current-supplying mould (CSM) and feeding large-section remelting electrode into its central part. Two variants of electric circuits of remelting electrode connection are proposed. In the first circuit the same potential is applied both to consumable and annular nonconsumable (CSM upper section) electrodes. In the second circuit, potentials of both the electrodes are different. The following technique of surfacing was proposed as a result of test surfacing performed with ANF-29 flux in CSM of 180 mm diameter with steel 40 electrodes of 40–130 mm diameter. After setting the slag pool in CSM, it is recommended to conduct the first stage (joining the base and deposited metal) with the first electric circuit. Electrode melting will be slower, but with optimum electric power applied to the slag pool through CSM, it is possible to achieve uniform penetration of base metal. Furtheron, at deposition of subsequent layers with higher efficiency and good quality of the deposited layer, one should proceed to the second electric circuit of remelting electrode connection. 8 Ref., 5 Figures.

Keywords: *ESS of end faces, large-section electrode, CSM, ESS electric circuits, base metal penetration, deposited metal formation, efficiency*

Quality of surfacing performed by any known method, particularly at joining metals with markedly differing properties, is largely determined by the ability to reach minimum and uniform penetration over the entire surface being joined. Otherwise, the problem of imparting special properties (wear resistance, thermal fatigue resistance, corrosion resistance, etc.) to the deposited metal is not completely solved. This is particularly important as regards relatively small thicknesses of the deposited metal. Depending on the method of electroslag surfacing (ESS), the proportion of base metal in the deposited metal is equal to 5–20 % [1]. Nonetheless, the main advantage of many ESS methods, alongside the high process efficiency, is the ability to deposit large metal masses.

In this case, preservation of preset special properties of the deposited metal across the deposited layer thickness does not cause any difficulties (particularly, in layers located far away from the fusion zone). Difficulties may arise in the bimetal fusion zone, because of a greater or smaller degree of mixing of the metals being joined and formation of intermediate structures with brittle components (martensite, carbide, nitride, and similar precipitates with different sizes and arrangement) in this zone, which markedly lower the joint mechanical strength, or promote formation of defects, most often cracks, already during surfacing. That is why this is exactly the problem which does not allow completely realizing all the advantages of the high-efficient process. A vivid example of such a situation is the so-called bulk ESS of teeth of mining shovel buckets [2]. This is good technology, which solves the major task of reconditioning expensive mining tools, but the surfaced (reconditioned) ladles are mostly used in operation for relatively easy to process rocks, when no increased impact loads are created.

It would seem that the simplest solution of this problem is performance of complex heat treatment of the bimetal product. This, however, is simply impossible to perform in most cases, because of absence of thermal furnaces with suitable dimensions and temperatures, and most importantly, the efficiency of the surfacing process becomes lower, and the rationality of its application is lost.

Thus, while the penetration depth is an important characteristic of any surfacing process (arc, plasma, etc.), it acquires special importance for ESS in the case of poor quality surfacing of large masses of often expensive metal. It should be noted that in this case removal of fusion zone defects also is a difficult-to-perform task.

The objective of the work is obtaining initial experimental data and selection of the direction of further studies to create a system of automatic regulation of quality at ESS of end faces with a large-section electrode in CSM.

At ESS in water-cooled devices-moulds wire or strip electrodes, or so-called large-section electrodes (bars, rods, etc. with up to 35000 mm^2 cross-sectional area) are usually used as electrodes. These technologies can be regarded as particular cases of the known and well-studied electroslag process — electroslag remelting (ESR). The difference consists only in that in the first case metal of a particular thickness is deposited on the billet surface, and in the second case

© Yu.M. KUSKOV, V.G. SOLOVIOV and V.A. ZHDANOV, 2017

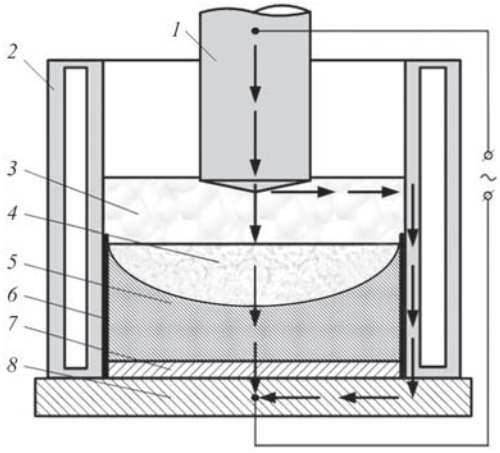

Figure 1. Metal pool shape at ESS (arrows show current distribution in the mould): *1* — electrode; *2* — mould; *3* — slag pool; *4* — metal pool; *5* — ingot; *6* — skull; *7* — seed; *8* — tray

the initial metal layer of ingot starts forming on the seed, which is a plate of 10–30 mm thickness. While for ESS, as we already noted, the penetration depth plays an essential role, at ESR the objective is just to achieve good fusion of seed and ingot metals, the more so since after remelting this lower (bottom) part of the ingot is removed (up to 15 % of ingot weight) [3]. For us it is important to assess formation of the metal pool (dimensions, depth) in a process similar to ESS, as it is exactly the heat transferred from the pool to the seed that determines heating and penetration of the latter.

It is seen from Figure 1 that the main thermal energy evolves under the electrode end face, imparting a specific cone-like shape to the metal pool. Accordingly, seed penetration is maximum along the ingot axis, with its decrease (or disappearance) along the ingot edges. From this analysis it follows that such an approach of metal joining cannot be applied to ensure high-quality surfacing.

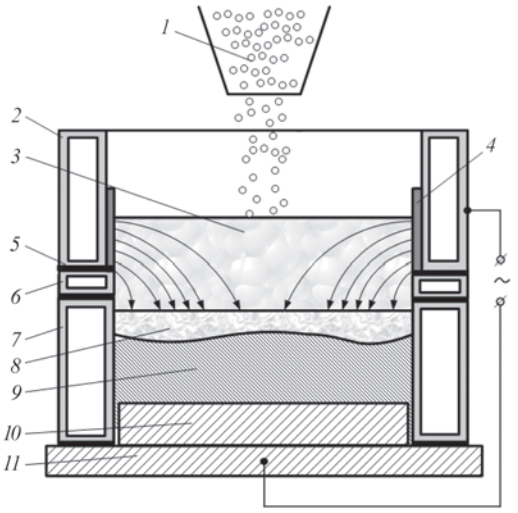

Figure 2. Shape of metal pool produced at ESS in CSM with discrete filler (arrows show current distribution in CSM): *1* — discrete filler; *2*, *6*, *7* — current-conducting, intermediate and forming sections of the mould, respectively; *3* — slag pool; *5* — insulating interlayer; *8* — metal pool; *9* — deposited metal; *10* — billet; *11* — tray

In order to eliminate this drawback, it can be promising to perform surfacing in CSM [4–7], which, essentially, is a sectioned nonconsumable electrode of annular type with voltage applied to its upper section. Such an electrode shape influences the nature of current distribution in the slag pool, respectively. Current from the wall of electrically supplying ring is partially flowing in the horizontal direction, but, mainly, it flows vertically to the processed surface of the billet. Here, its greater part flows directly in the near-wall area of the mould. This is confirmed also by the results of work [8] on simulation of the process of surfacing of end faces on conductive paper: approximately 50–90 % of current (depending on the distance from the mould wall) flows exactly in this area.

Figure 2 shows the shape of the metal pool obtained at surfacing in CSM with discrete filler, i.e. in the absence of a heat center in the middle of the mould, which is created by the electrode, as is usually the case at regular ESR.

It can be assumed that if we add the consumable surfacing electrode to CSM and distribute electric power between the annular nonconsumable electrode and consumable electrode in an optimum way, a minimum and uniform penetration of the base metal can be ensured.

We have conducted experiments on studying the applicability of one of the two electric circuits of consumable electrode connection in surfacing (Figure 3). According to the first circuit (Figure 3, *a*), the same potential is applied to electrodes of different type, and with the second one, the consumable electrode has a different potential.

Alongside achievement of minimum and uniform penetration of base metal, the quality of formation of outer surface of the deposited layer and deposition rate were taken into account as the criterion of optimality of the technology.

Experiments on surfacing were performed with a solid start in a stationary CSM of 180 mm diameter with electrodes of 40–130 mm diameter from steel 40. ANF-29 flux and alternating current were used.

Longitudinal sections were mechanically cut out of the surfaced billets, on which the fusion zone was studied after grinding and chemical etching. Appearance of surfaced billets (side surface and upper plane of the layer) was assessed visually.

Experiments on surfacing with the first (Figure 3, *a*) electric circuit (same potentials on electrode and CSM) showed the following. Melting of 90 mm electrode proceeds very slowly (compared to ESS process) at its immersion into the slag pool from 15 to 70 mm. Electrode melts only over its end face (side surface is not melted). No base metal penetration is observed. Deposited metal side surface has corrugations. In the case of application of larger diameter electrode (130 mm), the surfacing process proper and

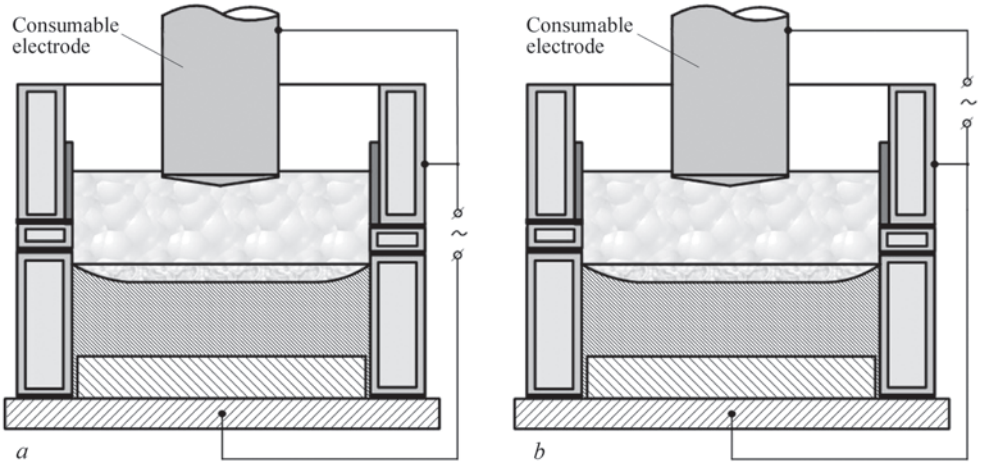

Figure 3. Electric circuits of remelting electrode connection at the same (*a*) and different from CSM (*b*) potential

its results are similar to those of surfacing with application of 90 mm electrode.

At surfacing with 40 mm electrode both accelerated melting of the electrode (at total applied power N = = 99 kV·A), and its delayed melting (N = 87 kV·A) are observed.

Apparently, stability of ESS process, speed of slag pool rotation, affecting the electrode melting and, eventually, process efficiency and surfacing quality, are largely determined by electric power N_{CSM}, applied to the slag pool through the CSM. Figure 4 shows the longitudinal macrosection of a bimetal billet, produced by surfacing with 40 mm electrode with N = 87 kV·A.

As follows from the results of surfacing with this electric circuit, at application of electrodes of different diameter no deep penetration of base metal is observed, either in the mould near-wall zone, not under the electrode. Therefore, such ESS circuit, in principle, allows creating a uniform thermal field, and, accordingly, similar penetration conditions over the entire surface of the billet being processed at appropriate optimum electric power applied through CSM. Another indirect confirmation of leveling of electric power across the mould cross-section and formation of a more flat metal pool in it is the increase of the speed of slag pool rotation at electrode removal from the slag due to redistribution of working current to the electrode and CSM in favour of the latter.

Surfacing with the second (Figure 3, *b*) electric circuit of remelting electrode connection showed the following results. First of all, this surfacing technology allows a significant increase of the efficiency of electrode melting process. So, at surfacing with 40 mm electrode the electrode melting rate rises up to 2–3 times, and at surfacing with 90 mm electrode — by approximately 2 times. Deposited metal formation and quality of the fusion zone substantially depend on surfacing mode. Figure 5 shows macrosections of a sample produced by surfacing with 90 mm electrode at different electric power of the process. At low power (N_{CSM} = 80–90 kV·A) «zero» fusion (by brazing type), formed under the impact of remelting electrode, is observed on 40 mm length in the central part of section, the other zones having deep penetration (≥20 mm) — Figure 5, *a*. This is accounted for by the fact that in this case the highest current was flowing from the annular nonconsumable electrode. Here, formation of the deposited layer side surface is unsatisfactory (presence of a large number of corrugations). At N_{CSM} = 130–135 kV·A (Figure 5, *b*) the central part of the section has small penetration (about 5 mm) on an approximately 50 mm length; in the other zones the fusion line has a lot of slag interlayers, without base metal penetration. Metal pool in the deposited metal has a relatively flat shape.

It follows from the above-said that surfacing by the technologies with different electric connection of the remelting electrode, can provide uniform and minimum penetration of base metal and allow achieving other criterial values at application of optimum electric power to the slag pool. Apparently, the following surfacing technique can be accepted for solving the defined problem. After setting the slag pool in the current-supplying mould (at solid or liquid start), the first circuit of remelting electrode connection should be used to conduct the first stage of surfacing (joining the base and deposited metals). Here, electrode melting will be delayed, but at optimum electric power applied to the slag pool through CSM, a uniform penetration of base metal can be achieved. Furtheron, i.e. at deposition of a thick layer, when it is necessary

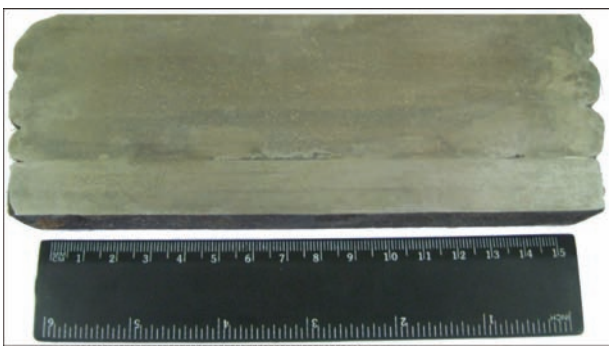

Figure 4. Longitudinal macrosection of bimetal billet, produced by surfacing with 40 mm electrode at N_{CSM} = 87 kV·A

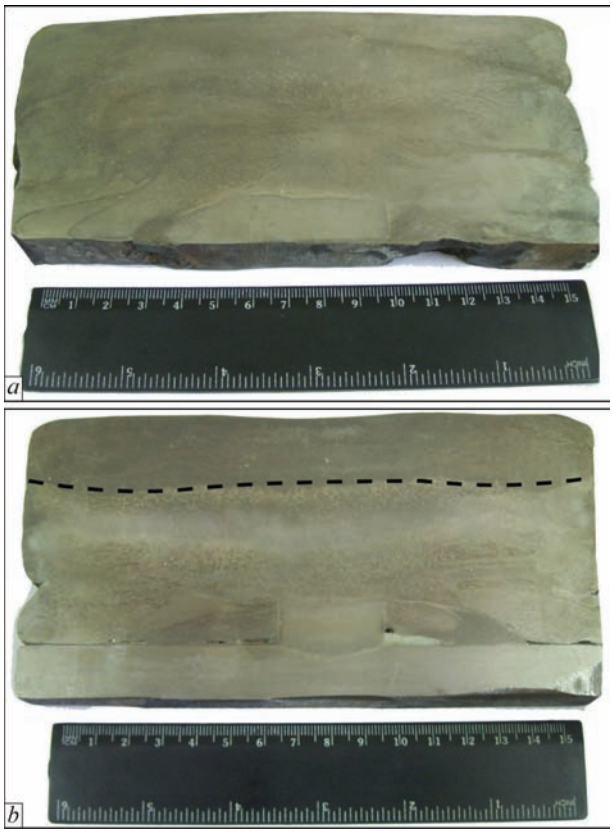

Figure 5. Longitudinal macrosection of a bimetal billet, produced by surfacing with 90 mm electrode at N_{CSM} = 80–90 (*a*) and 130 kV·A (*b*) (dashed line marks the shape of metal pool in the deposited metal)

to obtain higher process efficiency and high-quality surface of the deposited layer, the second circuit of electrode electrical connection should be applied.

On the whole, performed experiments showed that regulation of heat flows at ESS of end faces, both in the fusion zone, and at deposited layer formation is a complex task, solution of which depends on many parameters (both geometrical and electrical). Therefore, it is necessary to additionally perform a detailed, comprehensive investigation of this surfacing process. The following should be considered: application of other connection circuits, other number of power sources and kinds of applied current, application of not just remelting electrodes, but also nonsupplying consumable billets of different diameter, optimization of processed surface position relative to CSM current-supplying section.

Performance of such investigations will allow not only finding an optimum solution of the defined problem, but also creating prerequisites for automatic regulation of the process of ESS of end faces and obtaining the specified quality results even at deviation of the values of certain parameters from the initially assigned ones.

Conclusions

1. Unlike other surfacing processes, quality of electroslag surfacing with deposition of large masses of metal essentially depends on the fusion zone quality and to a smaller degree — on the quality of deposited metal proper.

2. The paper provides an analysis of the possibility of performance of ESS of end faces in the current-supplying mould with large-section electrode with application of two electric circuits — at the same and at different potential of the remelting electrode and CSM, in order not only to obtain minimum and uniform penetration of base metal, but also achieve high process efficiency with good formation of the deposited layer.

3. It is recommended to conduct the surfacing process at the first stage of metal joining by the technology, where the remelting electrode and CSM have the same potential. Furtheron, at deposition of subsequent layers, transition to the second electric circuit of remelting electrode connection should be made (electrode and CSM have different potentials). This will allow an essential increase of deposition rate with good formation of the deposited layer.

4. Proceeding from the performed studies, it was proposed to conduct a more comprehensive investigation of the process of ESS of end faces with large-section electrode. The following technological characteristics (both electrical and geometrical) were selected for consideration: electrode connection circuits, number of used power sources, kind of applied current, application of not just remelting electrodes, but also nonsupplying consumable billets, and position of the processed surface relative to CSM current-conducting section.

5. The final objective of the performed and planned investigations is formation of a data bank for developing a system of automatic regulation of the process of ESS of end faces and ensuring repeatability of surfacing quality results.

1. Kuskov, Yu.M., Skorokhodov, V.N., Ryabtsev, I.A. et al. (2001) *Electroslag surfacing*. Moscow, LCC Nauka i Tekhnologii [in Russian].
2. Ponomarenko, V.P.,Shvartser, A.Ya., Stroganova, G.V. (1985) Examination of fusion zone of high-chromium cast iron with high-manganese steel in electroslag surfacing. *Metallovedenie i Termich. Obrab. Metallov*, 11, 55–58 [in Russian].
3. Latash, Yu.V., Medovar, B.I. (1970) *Electroslag remelting*. Moscow, Metallurgiya [in Russian].
4. Frumin, I.I., Ksendzyk, G.V., Shirin, V.S. (1980) *Machine for electroslag remelting and surfacing*. USA Pat. 4185628 [in Russian].
5. Kuskov, Yu.M. Electroslag remelting in sectional current-supply mold. *Svarshchik*, **3**, 21–23 [in Russian].
6. Kuskov, Yu.M., Gordan, G.N., Bogajchuk, I.L. et al. (2015) Electroslag surfacing using discrete materials of different methods of manufacture. *The Paton Welding J.*, **5–6**, 30–33.
7. Kuskov, Yu.M. (2003) A new approach to electroslag welding. *Welding J.*, **4**, 42–45.
8. Tomilenko, S.V., Kuskov, Yu.M. (1999) Power specifics of electroslag process in current-carrying mold. *Avtomatich. Svarka*, **2**, 51–53[in Russian].

Received 20.09.2017

doi.org/10.15407/tpwj2017.12.06

IMPROVEMENT OF THE TECHNOLOGY OF PRODUCING EXTENDED COMPOSITE TRANSITION PIECES OF STEEL 20 — STEEL 08Kh18N10T MADE BY THE METHOD OF HOT SCREW ROLLING IN VACUUM*

B.V. BORTS, I.M. NEKHLYUDOV, N.D. RYBALCHENKO, V.I. SYTIN and **I.O. VOROBJOV****
NSC «Kharkiv Institute of Physics and Technology» of the NAS of Ukraine
1 Academichna Str., 61108, Kharkiv, Ukraine. E-mail: nsc@kipt.kharkov.ua

Changes in mill design using screw rolling in calibrated rolls were proposed and tested. Solid-phase welding in upgraded vacuum rolling mill was used to produce extended bimetal transition pieces with a helical texture that allows making sound solid-phase joints of more than 200 mm length of low-carbon steel and 08Kh18N10T steel. Investigation results were used to develop the technology of screw rolling in calibrated rolls. 12 Ref., 8 Figures.

Keywords: *vacuum screw rolling, extended tubular element of the transition piece, bimetal composites, upgrading*

Operating nuclear power plants of the second and third generations require improvement and extension of service life of piping in joints of dissimilar metals, which differ by their composition and properties, such as low-carbon steels with austenitic steels. Up to now such joints have been made in nuclear power plants by fusion welding, and are known to be the most susceptible to corrosion fracture.

In 2010–2012 during performance of a comprehensive «Resource» Program NSC KIPT developed new devices for solid-phase welding of composite materials by hot vacuum rolling in sheet rolling mill DUO-170 manufactured by KIPT [1, 2].

Developed technology of pack rolling of composite materials of steel 20 – steel 08Kh18N10T allows manufacturing circular transition inserts of different diameters, which have been introduced for long-term trials in the turbine department of Zaporizhya Nuclear Power Plant (ZNPP) and have demonstrated their performance under full-scale operating conditions.

Based on the developed technology of producing the new composite material, «Program of certification testing of composite welded joints of steel 20 – steel 08Kh18N10T made by solid-phase welding technology» was prepared, coordinated and approved in SC NEGC «Energoatom» in 2013.

During fulfillment of the comprehensive «Resource» program, it was found that composite transition inserts made by pack method, do not completely satisfy the needs of NPP technological documentation PNAE G-7-008-89 on dissimilar metal welding.

These deviations from the approved requirements of NPP technological documentation were the bases for substantiation of the possibility of upgrading the available equipment for vacuum screw rolling in calibrated rolls of extended transition elements from composite of steel 20 – steel 08Kh18N10T of 30 mm diameter and more than 200 mm length.

Analysis of experimental samples of extended transition pieces revealed several drawbacks of billets rolled in DUO-170 mill that necessitated development of the drawing for the design of a higher-capacity new mill DUO-175-2 with additional upgrading to eliminate these drawbacks.

Metal deformation and contact stresses in groove rolling. Rolling processes belong to high-efficient cost-effective methods of manufacturing metal products. Further development and improvement of these processes requires a comprehensive study of rolling parameters and ensuring optimum conditions of equipment operation.

In this connection, it is expedient to consider the distribution of deformations and contact stresses in rolling mill roll grooves during rolling, to establish the regularities of the change of contact tangential stresses and derive the dependencies for determination of

*Published be the materials of performance of targeted comprehensive program of NANU «Life and safety of structures, facilities and machines» («Resource») in 2013–2015.
**I.M. Korotkova, O.O. Lopata, O.T. Lopata participated in the work.

© B.V. BORTS, I.M. NEKHLYUDOV, N.D. RYBALCHENKO, V.I. SYTIN and I.O. VOROBJOV, 2017

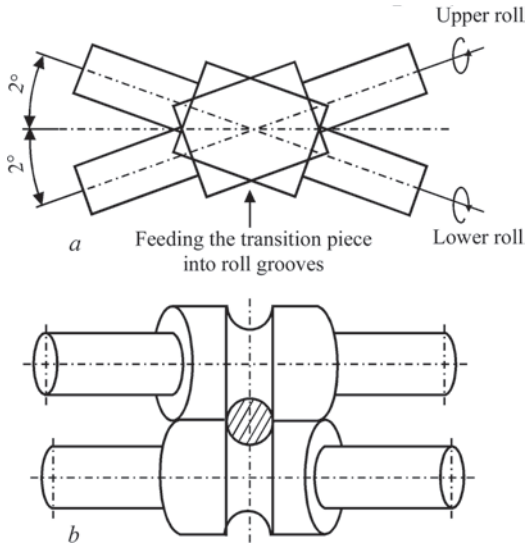

Figure 1. Schematic of roll positioning: *a* — plan view; *b* — end view

contact and total pressure of metal on the rolls, torque and position of neutral section in groove rolling. It is necessary to calculate the contact area in rolling in simple and complex grooves, as well as study the influence of outer zones on contact pressure in groove rolling, when $l/h_{av} < 1.5$ (l is the length of geometric center of deformation; h_{av} is the average height of deformation center).

Performance of comprehensive studies of industrial rolling mills [4-6] enabled establishing the values of metal pressure on the rolls, torques, energy parameters, forward slip, groove wear and accuracy of rolled stock dimensions. Mill reserves were revealed and recommendations on improvement of the technology of steel shape rolling were proposed.

Developed measures increase the productivity of rolling equipment, and improve the quality and accuracy of rolled stock dimensions.

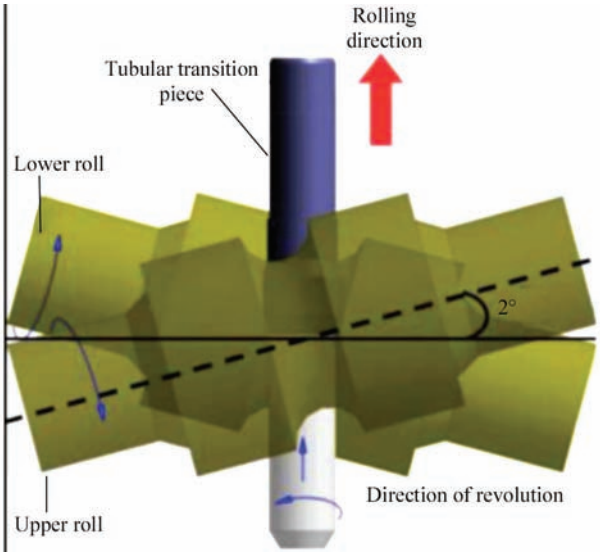

Figure 2. View of roll positioning and directions of motion during rolling (*top view*)

Mill upgrading. Mill upgrading consisted in determination of optimum calibration of roll bodies for rolling a round billet of 30 mm diameter, development of drawings and manufacturing new rolls with grooves, initially for 14.8 mm and then finishing the grooves in a semi-arc to 15.5 mm, to provide the finish diameter of 30 mm in the rolled and lathe-machined billet. Changes in groove size were due to a too large amount of metal flash on the horizontal slit of roll grooves. As it turned out after the first experiments on rolling the extended transition piece, the mill does not have the required rigidity (total deformation and sagging of rolls, screw gear of the stop screw). Nominal gap between the bodies of rolls brought together to metal contact, should be equal to 0.5–1 % of the body diameter, that is up to 1 mm on average. In the mill the roll return actually was equal to 2.3 mm. As a result, the outer layer of stainless steel turned into flash, and the uniformity of the composite outer layer was disturbed.

Analysis of experimental samples showed differences in the degree of deformation over the transition piece cross-section. Non-uniformity of deformation was determined from the data on microhardness of the components measured on templates of the cross-section of rolled billet of the transition piece of steel 20 – 08Kh18N10T composite. Microhardness was measured by Vicker's method at 25 g load in LM 700AT instrument of LECO. Non-uniformity of component deformation over the billet cross-section was also determined by measurement of the size of component grains to the rolling direction [2, 7].

In order to reduce the found drawbacks, during improvement of the technology of producing extended transition elements, it was envisaged to perform compression with screw rolling that provides the helical texture. For this purpose, drawings were developed, manufacturing and mounting of grooved rolls in the mill was performed not in the traditional position, normal relative to the rolling direction, but with each roll turned at an angle of 2° to the axis of mounting the rolls in DUO-170 mill and facing in opposite directions (Figures 1, 2).

Thus, the rolls were turned by 4° relative to each other, that should make the billet additionally rotate around its axis during forward motion at the moment of rolling. This should provide reduction of material loss as flash due to increase of the zone of its texture displacement along a helix (Figures 3, 4).

Changes of roll position led to additional changes in the design of the run-in and run-out chutes (see Figure 5), which were made, allowing for the arising forces of torque on the sample during movement of the billet being rolled, as well as to essen-

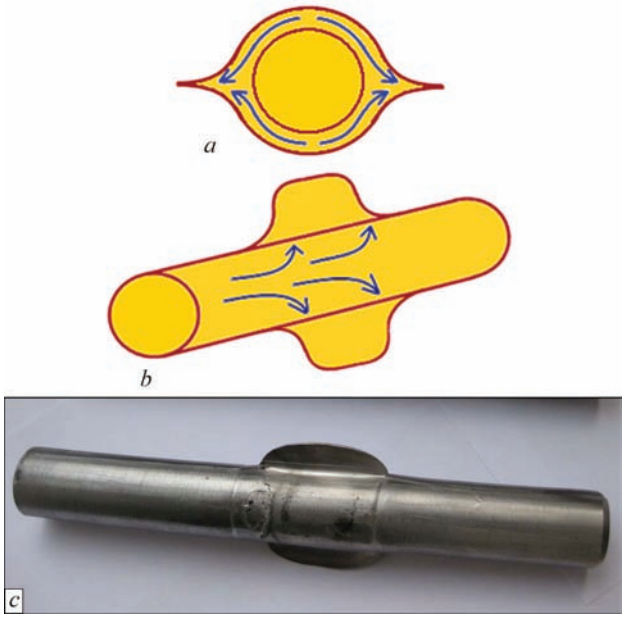

Figure 3. Direction of metal flow (*a*, *b* — schematic from sample end face) at application of parallel rolls (*c*)

tial changes in the design of the fastening of roll chocks to bearings.

Changes in the transition piece billet design were additionally made, namely two grooves are first cylindrical and then conic, as well as in the design of the tip of rod billet of steel 20 to achieve its tighter fitting in the initial billet body. These changes prevent the billet rod being pushed out at the initial moment of rolling when entering the roll grooves.

Unlike the previous experiments, when rolling was performed in the mill without helical motion, in the mill with screw rolling the inlet cone on the transition piece billet was changed from 45 to 25° for better gripping of the billet by rolls.

Making samples of an extended transition piece by the improved technology and quality control. Testing on model material — aluminium was performed to assess the mill performance during rolling of extended transition elements in rolls with screw rolling by the new procedure. The billet was made by drawings of the composite transition piece.

Testing of the new rolling technology confirmed the possibility of providing axial rotation of the billet

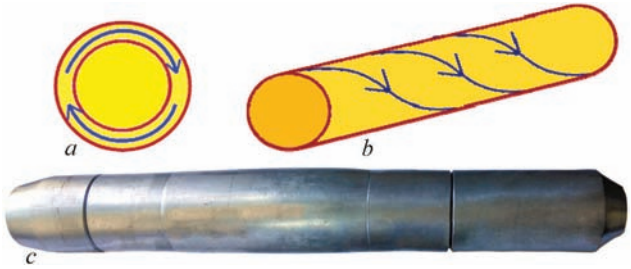

Figure 4. Direction of metal flow at screw rolling with application of helical texture: *a* — sample end view; *b* — general view of texture; *c* — test sample from aluminium

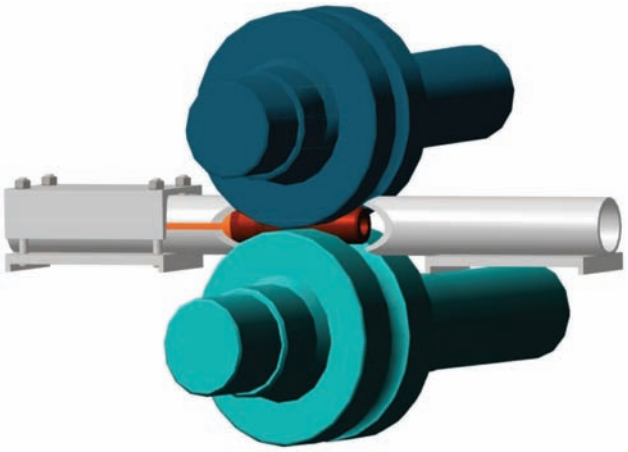

Figure 5. Positioning of grooved rolls with guides

in combination with its simultaneous forward motion during rolling at solid-phase joining of the transition piece components.

As shown by experiments, rolling of extended transition piece by the improved technology with screw rolling proved to be correct.

Produced experimental samples had helical texture that provides uniform compression of the material around the total perimeter of the billet in the sites of solid-phase joining of two dissimilar materials (Figure 6).

Conducting non-destructive ultrasonic testing of manufactured extended tubular transition pieces from steel 20 – 08Kh18N10T. Among the many methods [8] of conducting ultrasonic testing (UT) selection of a particular one should be based on the maximum possibility of defect detection. Appearance of the tested sample is given in Figure 6, *b*. The work was performed using ultrasonic flaw detector UD4-76.

For extended tubular transition pieces of steel 20 – 08KhN10T two procedures were selected, namely echo-method using combined direct piezoelectric transducers (PET) with 2.5 MHz frequency and echo-mirror method.

Before UT the instrument was calibrated on test standard defective and sound samples using both direct and inclined PET. In case of the presence of a defect when using echo-mirror UT, the amplitude of the transition region signal will be higher than that of the transition zone of sound standard test sample. In case

Figure 6. Extended tubular element made in DUO-175-2 mill; *a* — before rolling; *b* — after rolling and machining

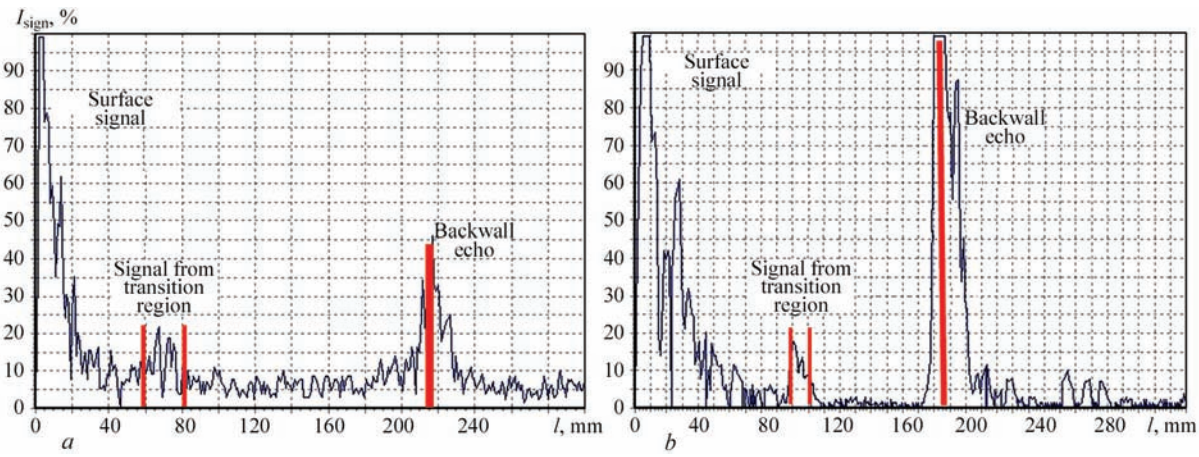

Figure 7. Oscillogram of the transition region of test sample from steel 20 – 08Kh18N10T (echo-method): *a* — from the side of 08Kh18N10T steel; *b* — from the side of steel 20

of application of UT echo-procedure, the transition region signal should be compared with the backwall echo of the studied sample. Presence of a defect will be indicated by backwall echo signal amplitude that is higher than that of transition region signal.

Results of UT of extended tubular transition pieces by the echo-method are given in Figure 7, and those of echo-mirror method are shown in Figure 8. As one can see from the oscillograms, defects in the form of cracks, voids or unwelded areas are absent both in the body and on the boundary of the components.

Development of technological instructions on solid-phase welding of extended transition pieces with outer sleeve from 08Kh18N10T steel and inner rod from steel 20. To ensure compliance with the requirements of NPP technological documentation PNAE G-7-008-89 [9] technical documentation has been developed on manufacture of extended composite transition pieces, which contains technological instructions on operating sequence for solid-phase joining of transition elements from dissimilar metals by the method of hot vacuum rolling. A series of mandatory testing on quality control has been specified in keeping with the requirements.

The instructions give the following list of such manufacturing stages:

- process of initial material preparation: machining of the sleeve and rod from steel 20 before assembly into the initial billet before rolling and assembly of the packs for rolling;
- process of joining the transition piece elements in vacuum rolling mill DUO-175;
- safety requirements during joining of the components of composite transition pieces;
- final operations after producing the transition element;
- quality control of the joint of the components in the finished product.

As the main conditions for producing composite transition pieces were providing high strength and tightness, quality of the made products was assessed based on the requirements of the main document of control rules (CR) requirements for NPP equipment and piping, welded joints and surfaced parts PNAE G-7-010-89 [10].

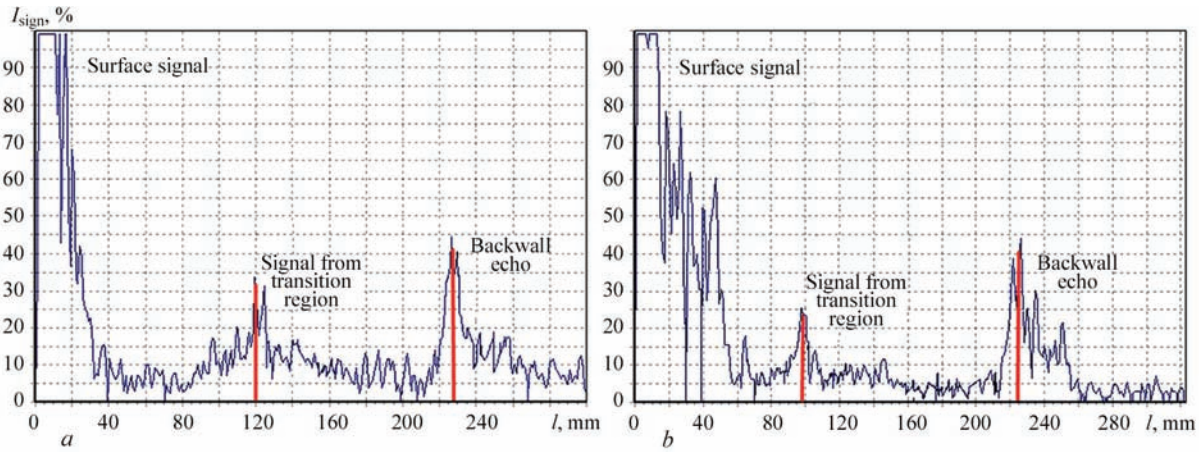

Figure 8. Oscillogram of the transition region of test sample from steel 20 – 08Kh18N10T (echo-mirror method): *a* — from the side of 08Kh18N10T steel; *b* — from the side of steel 20

CR data are the guidelines for design, development, manufacture and mounting of equipment and piping, and they specify the procedure, kinds, scope and methods of control and criteria for assessment of the quality of welded joints and surfaced parts (products).

In keeping with CR requirements as per PNAE G-7-010-89 the following kinds of testing are envisaged for our products:

- nondestructive method of ultrasonic testing on the surface in the area of joining layers of dissimilar metals in keeping with GOST 14782–86 [11];
- tightness control by hydraulic testing at filling of the tubular billet inner part with liquid (water) under pressure and soaking for a day under up to 200 bar pressure;
- mechanical shear strength testing of layers of the composite components in keeping with GOST 14759–69 [12] for adhesive joints of sheet materials;
- metallogrpahic studies of tightness and length of the joint boundary as well as layer thickness and degree of structure deformation in the zone of the component metal joint.

Quality control is performed as follows: in keeping with item 1 — 100 % pieces in the batch; in keeping with item 2 (hydraulic tightness tests) — one sample from a batch after 100 % UT; in keeping with items 3, 4 — one product from the transition piece batch.

Conclusions

1. A design of rolling mill assemblies was developed and upgraded that allowed producing extended tubular transition pieces for NPP due to rotation of the piece during rolling.

2. Mock-up samples of extended tubular transition pieces after rolling demonstrated screw structure along the sample surface, as well as absence of billet curvature when using upgraded rolls, mounted at an angle to each other.

3. Design, manufacture and additional upgrading of new higher-capacity vacuum mill DUO-175-2 instead of badly worn mill DUO-170, enables producing higher quality transition pieces from steel 20 with stainless steel of 08Kh18N10T type, which are intended for introduction in nuclear power stations.

4. Nondestructive ultrasonic testing showed absence of defects in the bod and on the boundary of the components.

5. Procedures of quality control of the transition elements, in keeping with the rules of control of «Equipment and piping of nuclear power plants, welded joints and clad products. Control rules» (PNAE G-7-010-89) were developed and technological instructions on solid-phase welding of extended transition pieces with outer sleeve from 08Kh18N10T steel and inner sleeve from steel 20 were prepared.

1. Zemzin, V.N. (1991) Welded joints of dissimilar steels. In: *Welding and welded materials*. Vol. 1. Moscow, Metallurgiya, 422–442 [in Russian].
2. Borts, B.V., Boevodyn, V.M., Neklyudov, I.M. (2012) Increase of service life of NPP piping due to application of the extended composite inserts from dissimilar materials. In: *Problems of life and safety service of structures, constructions and machine*. Kiev, PWI, 154–158 [in Ukrainian].
3. Shavlakov, A.V. et al. *Program of qualification test of composite welded joints of steel 20-steel 08Kh18N10N produced by technology of solid-phase welding*. Sheet 15-31/4323. Approv. 25.06.2013 [in Russian].
4. Tselikov, A.I. (1962) *Theory of calculation of efforts in rolling mills*: Refer. Book. Moscow: Metallurgizdat [in Russian].
5. Tarnovsky, I.Ya., Levanov, A.N., Poksevatkin, M.I. (1956) *Deformation of metals in rolling*. Sverdlovsk, Metallurgizdat [in Russian].
6. Polukhin, P.I., Vorontsov, V.K., Kudrin, A.B. et al. (1974) *Strains and stresses in metal forming*. Moscow, Metallurgiya [in Russian].
7. Borts, B.V., Boevodin, V.M., Neklyudov, I.M. et al. (2013) Application of solid phase joints for increase of reliability of piping of 2nd and 3rd generation reactors. *Nauka i Innovatsii*, 9(**2**), 10–17 [in Russian].
8. Samojlovich, G.F. (1976) *Nondestructive testing of metals and products*: Refer. Book. Moscow, Mashinostroenie [in Russian].
9. *PNAE G-7-008–89 (DNAOP 0.04-1.05–90)*: Rules of arrangement and safety service of equipment and piping of nuclear power plants [in Russian].
10. *PNAE G-7-010–89*: Equipment and piping of nuclear power plants, welded joints and deposits, rules of inspection [in Russian].
11. *GOST 14782–86:* Nondestructive testing. Welded joints. Ultrasonic methods [in Russian].
12. *GOST 14759–69.* Glues. Method of determination of shear strength [in Russian].

Received 02.10.2017

doi.org/10.15407/tpwj2017.12.07

IMPROVEMENT OF IMPACT TOUGHNESS OF METAL OF COMBINED WELDED JOINTS OF ALLOYED BAINITE STEELS

S.I. MORAVETSKY[1], **A.K. TSARYUK**[1], **A.V. VAVILOV**[2] and **A.G. KANTOR**[2]
[1]E.O. Paton Electric Welding Institute of the NAS of Ukraine
11 Kazimir Malevich Str., 03150, Kiev, Ukraine. E-mail: office@paton.kiev.ua
[2]PJSC «Turboatom»
199 Moscow Ave., 61037, Kharkov, Ukraine. E-mail: office@turboatom.com.ua

A possible approach in the development of technology of producing combined welded joints of bainite steels was formulated as-applied to critical welded units, based on the purposeful presetting the optimum content of alloying elements and impurities in the base and filler metal within their grade composition according to the standard documents and contributing to improvement of their service characteristics. The comparison of results of experimental investigations obtained within the standard certification of welding technology, allows assuming that the implemented approach is effective. 9 Ref., 2 Tables.

Keywords: *alloyed steel, rotor steel, combined welded joints, welding consumables, chemical composition, submerged arc welding, heat treatment, tempering brittleness, impact toughness*

In the PJSC «Turboatom» the new generation steam turbine K-325-23.5 was manufactured, which meets the modern requirements to reliability, economy and maneuverability [1]. For this turbine a forge-welded combined rotor of medium-pressure cylinder was designed, operating in a high- and low-temperature mode [2]. A part of the rotor operating in the high-temperature mode (1–11 stages) is manufactured of steel EI 415 (20Kh3MVFA). A part of the rotor, operating in a low-temperature mode (12–16 stages) is manufactured of steel 25Kh2NMFA. These steels belong to the same structural class, but differ in the alloying system. In steel EI 415 the nickel content is 2.6 times lower than in 25Kh2NMFA, and the chromium is 1.5 times higher. Moreover, steel EI 415 contains the strong carbide-forming elements: vanadium and tungsten. Due to the mentioned features of alloying, the steel EI 415 has a higher phase stability at elevated temperatures, which determines its selection for manufacture of a rotor section operating in a high-temperature mode.

Earlier, the technology for producing a combined welded joint of steel EI 415 and 25Kh2NMFA (further — joint EI 415 + 25Kh2NMFA) was developed using the wire of grade Union S 3 NiMoCr (type A-S 55 4 according to ISO 26304) in combination with flux of grade UV 420 TT (type SA FB 1 65 DC according to ISO 14174). It is based on the approach, in accordance with which the homogeneous welded joints of steel 25Kh2NMFA are produced: filling the U-shaped groove of a constant width by a multipass submerged arc welding method with preheating the base metal to 350 °C and the postweld high tempering for 40 hours at the.630 °C temperature. However, the results of research certification of this technology showed that the tempering temperature, optimal for the metal of weld fusion zone with steel 25Kh2NMFA appeared to be insufficient to provide the required impact toughness of metal of weld fusion zone with steel EI 415, regardless of the used welding consumables [2]. Thus, at the 20 °C temperature, the average value of *KCV* of weld metal of welded joint steel EI 415 (notch along the fusion zone), was 42 J/cm^2. This value is lower than the required value of impact toughness ($\geq$ 59 J/cm^2) for the metal of homogeneous welded joints of steel 25Kh2NMFA, established by technical documentation on manufacturing the rotors of turbines and a priori widespread for the joints EI 415 + 25Kh2NMFA.

Therefore, the further aim was to find technological capabilities for increasing *KCV* of metal of the fusion zone on steel EI 415 to the required value. Moreover, it is desirable to preserve the process of welding steels 25Kh2NMFA and EI 415 between each other as a homogeneous joint, which is characterized by simplicity (without preliminary surfacing to the edge of the base metal, intermediate heat treatment, etc.). To achieve this aim, the analysis of the previously obtained results of research certification of the technology of welding the joints EI 415 + 25Kh2NMFA was carried out [2]

© S.I. MORAVETSKY, A.K. TSARYUK, A.V. VAVILOV and A.G. KANTOR, 2017

in comparison with specific welding conditions of the certified reference welded joint (RWJ) and the known regularities of changing mechanical properties during tempering of alloyed steels.

The results of investigations [3–6] allow assuming that the most obvious cause for the lowered impact toughness of the fusion zone on steel EI 415 is a tempering brittleness. It is known about negative influence of harmful impurities, especially phosphorus, on the tendency of low- and medium-alloyed steels to embrittlement. In particular, the harmful effect of phosphorus, introduced together with manganese at the content of latter being 1 % and higher, sharply manifests itself. Similarly to manganese, silicon also increases the tendency of steels to tempering brittleness. Moreover, the increase in silicon content expands the dangerous range towards the high temperatures.

It was generalized, that for the most considered steels, for developing the phenomena of tempering brittleness the temperature range of 250–650 °C can be considered [4–6]. Within this range, there are temperatures of preliminary and concurrent preheating, in which the welding of rotor steels is usually carried out in order to produce the minimum content of products of the diffusion-free decay of austenite in the HAZ metal and to prevent the delayed fracture of welded joints.

During tempering of welded joints of rotor steels, it is also impossible to avoid their staying in a dangerous temperature range, as far as for thick-walled large-sized welded units after holding at the tempering temperature, only slow furnace cooling is possible. Therefore, in principle, for any area of welded joint of any rotor steel after heat treatment some embrittlement and a corresponding reduction in impact toughness is inevitable as compared to the level which could be achievable at the accelerated cooling of rotors after tempering.

In case of carrying out tempering of welded joint of rotor steel at the optimum temperature (above the temperature range of embrittlement of this steel), the final stage of embrittlement of welded joint metal turns to be low, since it is determined only by the holding time in the dangerous range when the product is subjected to the furnace cooling. This is confirmed by the practice of producing homogeneous welded joints of steel 25Kh2NMFA, after the tempering of which at 630 °C during 40 h, the requirement to impact toughness *KCV* ($\geq$ 59 J/cm^2) of the fusion zone metal is provided with a noticeable margin. At the same time, for steel EI 415 the lower limit of the recommended tempering temperatures according to TS 108-1029–81 is 660 °C. Therefore, it can be assumed that the accepted temperature of tempering the joints EI 415 + 25Kh2NMFA (630 °C) enters the dangerous range for steel EI 415. In this case, the metal of fusion zone on steel EI 415 is in the dangerous range at all the stages of producing welded joint (preliminary and concurrent preheating during welding, transportation to the furnace, heating, holding at the temperature of high tempering and furnace cooling). Then, the lowered values of impact toughness of the metal of fusion zone on steel EI 415 in the combined joint and also revealed by mechanical tests, are, apparently, the logical result of its many-hour holding in a wide range of temperatures, where in steel EI 415 the totality of phenomena of tempering embrittlement of a different nature can develop.

It is possible to eliminate the embrittlement of steel EI 415 and the metal of all the zones of its welded joint only by tempering above the dangerous range, i.e. at the temperatures recommended for it ($\geq$ 660 °C). But the carrying out of the postweld tempering of joints EI 415 + 25Kh2NMFA at the temperatures $\geq$ 660 °C is unacceptable, since it leads to weakening the steel 25Kh2NMFA [6], the tempering temperature of which is 630–650 °C according to TS 108-995–81. If there is no possibility to increase the temperature of postweld tempering of the combined rotor, it is only possible to influence other factors determining the tendency of steel EI 415 to tempering embrittlement, its chemical composition and duration of metal staying in the dangerous range.

The features of steel EI 415, selected for manufacturing the high-temperature part of the combined rotor of the steam turbine K-325-23.5 for the Uglegorsk TPS, unlike the steel applied in the previously certified RWJ [2], were a very low phosphorus content and the content of silicon, reduced to the minimum (Table 1).

The duration of metal staying of combined welded joint in the most dangerous area in the range of embrittlement of steel EI 415 was reduced by establishment of rigid requirements to the temperature of concurrent heating, control of the temperature of base metal during welding in the vicinity of the groove and its active regulation due to change in the power of heating device to prevent overheating. As a rule, the lower limit of the temperature of preliminary and concurrent preheating of the combined welded joint EI 415 + 25Kh2NMFA as 350 °C is appointed. At the positive ambient temperature in the course of continuous automatic welding of circumferential joint, the temperature of the metal as a result of automatic heating begins to exceed the preset temperature rather soon. In view of the notion of the required temperature of preheating the steel EI 415 (400–500 °C), which has long been formed in the practice of welding the homogeneous joints of this steel [7, 8], the effect of self-heating of metal of the joint EI 415 + 25Kh2NMFA was not still considered undesirable.

Table 1. Content of elements in steel EI 415 (TS 108-1029–81) in the composition of RWJ EI 415 + 25Kh2NMFA and in metal of their welds, wt.%

Object of control	C	Si	Mn	Ni	Cu	Cr
Steel EI 415 according to TS 108-1029–81	0.17–0.24	≤ 0.40	0.25–0.60	≤ 0.50	≤ 0.25	2.40–3.30
Steel EI 415 in RWJ, certified in 2011 [2]	0.22	0.27	0.32	0.30	0.12	3.14
Steel EI 415 in RWJ, certified in 2014	0.23	0.059	0.35	0.38	0.15	2.71
Weld metal in RWJ, certified in 2011 [2]	0.088	0.32	1.61	2.31	–	0.44
Weld metal in RWJ, certified in 2014	0.088	0.37	1.41	2.31	–	0.72

Table 1 (cont.)

Object of control	Mo	V	W	S	P
Steel EI 415 according to TS 108-1029–81	0.35–0.55	0.45–0.70	0.30–0.50	≤ 0.022	≤ 0.025
Steel EI 415 in RWJ, certified in 2011 [2]	0.40	0.66	0.40	0.010	0.012
Steel EI 415 in RWJ, certified in 2014	0.41	0.50	0.32	0.003	0.005
Weld metal in RWJ, certified in 2011 [2]	0.60	–	–	0.009	0.022
Weld metal in RWJ, certified in 2014	0.50	0.018	–	0.012	0.017

Therefore, in the process of filling the deep groove, the temperature of the .concurrent preheating of weld metal and the areas of the base metal adjacent to it could amount to 400–450 °C or higher for a long time. This mainly concerns the full-scale model of the rotor, containing RWJ EI 415 + 25Kh2NMFA, on which the certified welding process is reproduced. The differences in values of weight and dimensions and heat capacity of the rotor and its full-scale model contribute to a particularly strong overheating of the latter (up to the maximum values of the above-mentioned temperature range).

Meanwhile, from the point of view of the known facts, holding the metal of the joint welded of alloyed steels in this range can lead to undesirable consequences. At first, it enters the range of reversible tempering brittleness of steels at 375–575 °C [5]. Secondly, due to excessively low cooling rate $w_{6/5}$ and elevated temperature of austenite decay, the unfavorable changes in composition of the decay products can occur. The γ-phase is stabilized and the content of residual austenite grows. Except of bainite and martensite, ferrite may also appear [9]. This means nothing more than an increase in the degree of microchemical (phase) heterogeneity of metal of the overheating area and it adversely affects its mechanical properties and tendency to delayed fracture.

Therefore, in the scopes of production certification of the technology (before welding the rotor for the Uglegorsk TPS), in the course of welding of RWJ EI 415 + 25Kh2NMFA, the measurement of temperature of the concurrent preheating was combined with the change in the power of gas heater flame (as required). Due to regulation of gas heater power, all the values of temperature of preliminary and concurrent heating of the RWJ metal, measured during multipass welding, were in the range of 316–365 °C.

Thus, all the changes in the previously developed technology of welding the joints EI 415 + 25Kh2NMFA consisted only in the mentioned limitation in top of the temperature range of the concurrent preheating and differences in the chemical composition of base metal of steel EI 415 in the certifying RWJ presented in Table 1. The other conditions and parameters of welding technology, methods of investigation of mechanical properties of RWJ metal, schemes of cutting out the specimens for impact bending tests remained unchanged and described in detail in the work [2].

The results of evaluation of impact toughness of the RWJ metal sections produced during the production certification of changed welding technology are shown in Table 2 in comparison with the similar results of research certification [2]. The combined effect of change in the temperature of concurrent preheating and the content of silicon and phosphorus in the base metal of steel EI 415 appeared to be quite effective. The average value of impact toughness of the welded joint metal (notch along the fusion zone of weld and steel EI 415) increased almost twice. The difference in the content of phosphorus and especially manganese in the weld metal of the RWJ, certified according to the changed technology, can be considered negligible as compared to the similar values according to the research certification results (see Table 1). Then the marked increase in the average value of *KCV* of the weld metal (notch in weld height) by 68 % can be explained almost exclusively due to the favorable effect of changed thermal mode of the multipass welding.

The obtained values of *KCV* with a reliable margin meet the requirement to impact toughness (≥ 59 J/cm^2) of metal of the combined welded joint of rotor steels at a room temperature. All the other characteristics of mechanical properties of any section of RWJ EI 415 + 25Kh2NMFA, produced applying the changed technology, also meet the specified requirements.

As one of the results of the gained experience of welding the combined rotor steels, it is appropriate

to note the role and generalize the approach realized above, which, in a number of cases, can apparently be very productive both in independent application as well as in combination with other technological measures. This approach, according to which the search for reserves to approximate the controlled characteristics to the required value is carried out in the ranges of the content of alloying elements and impurities in steels, admitted by regulatory documents [6]. This way can be the most rational for improvement of the technology for producing the combined welded joints of two bainite steels, for example, when the ranges of optimum temperatures of their tempering do not match and it is impossible to provide meeting the separate characteristics to the required values applying postweld tempering, and the degree of discrepancy is low. The realization of the mentioned approach should consist in the fact that the postweld tempering of the combined joint «steel 1 + weld + steel 2» is carried out at the temperature, guaranteeing the proper mechanical properties of all the areas of welded joint of steel 1. Moreover, on the basis of general knowledge about the effect of alloying elements and impurities on the controlled characteristic, the most favorable chemical composition of steel 2 is established (however, within the limits of its standard grade composition) and the coordination of more rigid requirements to the content of one or more elements with the manufacturer of this steel is carried out.

The same may concern the deposited metal, and in this case, special requirements to the content of alloying elements are coordinated with the manufacturer of welding consumables. There is a positive experience of such coordination, during which an enterprise-supplier of the wire of grade Union S 3 NiMoCr expressed its readiness to provide its chemical composition within the welding frames of ISO 26304, but in the required more narrow limits.

Conclusions

1. The technological approach was formulated, which can be useful in improvement of technology for producing combined welded joints of bainite steels. If the postweld tempering of a combined welded joint of the mentioned steels at a temperature higher than the embrittlement range of one of these steels is impossible, it is possible to reduce the tendency to tempering embrittlement and ensure the correspondence of impact toughness of metal of the fusion zone of this steel to the required values by limiting the content of silicon in this steel and (or) manganese in the .scopes of standard graded composition of steel, as well as phosphorus.

2. The preheating of metal of the combined welded joints of steels EI 415 and 25Kh2NMFA to the temperature of 350 °C and preventing its overheating in multipass submerged arc welding above 365 °C (welding at the temperature of the .concurrent preheating considerably lower than that, which was still considered necessary for steel EI 415) has a favorable effect on the impact toughness of the overheating area on steel EI 415.

3. The results of investigations in the frames of the production certification of the technology of submerged arc welding of the combined joint of steels EI 415 and 25Kh2NMFA confirmed the suitability of the certified technology for manufacture of the combined rotor of a medium-pressure cylinder of the steam turbine K-325-23.5 for thermal power stations (TPS).

1. Subotin, V.G., Levchenko, E.V., Shvetsov, V.L. et al. (2009) *Development of steam turbines of new generation of 325 MW power*. Kharkiv, Folio [in Ukrainian].
2. Tsaryuk, A.K., Moravetsky, S.I., Skulsky, V.Yu. et al. (2012) Development of forge-welded combined medium-pressure rotor for 325 MW steam turbine. *The Paton Welding J.*, **8**, 36–41.
3. Goldshtejn, Ya.E. (1963) *Low-alloyed steels in machine-building*. Moscow-Sverdlovsk, MAShGIZ [in Russian].
4. Braun, M.P. (1965) *Complexly-alloyed structural steels*. Kiev, Naukova Dumka [in Russian].
5. Novikov, I.I. (1978) *Theory of heat treatment of metals*: Manual. Moscow, Metallurgiya [in Russian].
6. Zemzin, V.N., Shron, R.Z. (1978) *Heat treatment and properties of welded joints*. Leningrad, Mashinostroenie [in Russian].
7. Timofeev, M.M., Vasilchenko, G.S. (1962) Development of discs from dissimilar steels for gas turbine EGTU 1000. Problems of welding in power machine-building. In: *Transact. of TsNIITMASH*. Book 104. Ed. by L.M. Yarovinsky. Moscow, MAShGIZ, 100–109 [in Russian].
8. German, S.I. (1972) *Electric arc welding of heat-resistant steels of pearlitic class*. Moscow, Mashinostroenie [in Russian].
9. Shorshorov, M.Kh, Belov, V.V. (1972) *Phase transformations and changes of properties in welding*: Atlas. Moscow, Nauka [in Russian].

Received 22.09.2017

doi.org/10.15407/tpwj2017.12.08

DEVELOPMENTS IN THE FIELD OF LASER WEDLING EQUIPMENT AND TECHNOLOGIES PERFORMED AT E.O. PATON ELECTRIC WELDING INSTITUTE (Review)*

V.D. SHELYAGIN, A.G. LUKASHENKO, V.Yu. KHASKIN, A.V. BERNATSKY, A.V. SIORA, D.A. LUKASHENKO and **I.V. SHUBA**
E.O. Paton Electric Welding Institute of the NAS of Ukraine
11 Kazimir Malevich Str., 03150, Kiev, Ukraine. E-mail: office@paton.kiev.ua

The paper provides a review of a series of developments of E.O. Paton Electric Welding Institute performed in course of the latest years in the field of laser welding equipment and technologies. These developments were tested or implemented in commercial production at the enterprises of People's Republic of China in Changchun and Harbin and in Ukraine in Kiev, Chernovtsy and Dnipro. The spheres of application and factors limiting the tendency of fast development and implementation of laser welding technology at Ukrainian enterprises have been outlined. 11 Ref., 12 Figures.

Keywords: *laser welding, technology development, development of apparatus and fixture, laser technological complexes, welded joints, mechanical properties*

Global tendency of the world's progress in the economy of the most developed countries is widespread application and improvement of new science-based perspective technologies, for example, such as laser ones [1–5]. Application of laser technologies is critical for rising a labor productivity and competitiveness of economy. Distinguishing features of laser application in production is high quality of received products, high productivity of the processes, saving of human and labor resources, ecological cleanness.

The lasers with such unique properties as high concentration of radiation power, coherence and monochromaticity have found wide application in aircraft-, rocket-, shipbuilding [5–8] and car construction [8] etc. branches of industry, science, engineering, communication, medicine, biology and other fields. Figure 1 shows an analysis of the world's market volumes of realization of laser radiation sources (without consideration of accompanying components, technological and other fixture) in 2013–2016 and prediction for 2017 [4]. According to data of reputable core publication «Laserfocusworld» the laser engineering market shows steady growth in the last five years and its annual volume has already exceeded 10 bln of USD. At that portion of laser radiation sources, used for material processing, makes around 30 %. (Figure 2) [2]. In turn, the main technological operations of material processing, in which laser radiation is used, are cutting (35 %), welding (25 %), microprocessing (20 %) and engraving (15 %) [3].

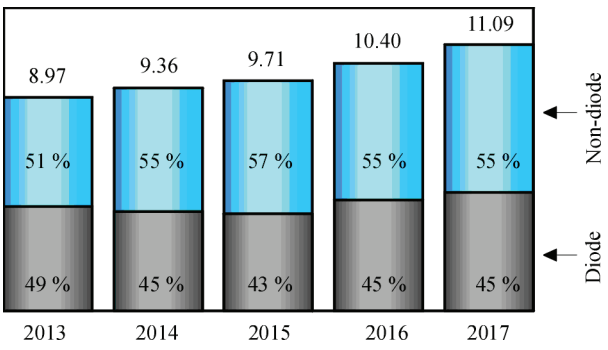

Figure 1. Sales indices (in bln of USD) of world market of laser units in 2013–2016 (without consideration of manipulators and fixture) and prediction for 2017 [4]

Analysis of the international market of laser technologies [1] allows detecting the main tendencies of its development. Among them are:

- high portion of equipment input costs in total volume of market of laser technologies;
- maintenance of laser technologies business in the countries of Western Europe, USA and others market-economy countries that reflects the need in high-qualified personnel;
- high cost of laser technological equipment resulting in reduction of consumer demand in equipment with improved process characteristics;
- increase of portion of services due to rise of complexity of laser technological systems that re-

*By materials of a report made at VIII International Conference on «Beam Technologies in Welding and Materials Processing», September 10–16, 2017, Odessa.

© V.D. SHELYAGIN, A.G. LUKASHENKO, V.Yu. KHASKIN, A.V. BERNATSKY, A.V. SIORA, D.A. LUKASHENKO and I.V. SHUBA, 2017

quires high efforts and expenses for their installation, development and maintenance as well as presence of high-qualified service staff;

● recruiting mainly outside organizations for performance of functions related with application of laser technologies.

All mentioned above tendencies are typical for the market of laser technologies used in material processing in Ukraine. Besides, it should be noted that the most typical additional factors limiting development of laser technologies market in Ukraine, are:

● absence of domestic producers of modern powerful laser units for material processing;

● loss of technologies for consumables manufacture (optical; power; electron and other elements), which were developed and implemented into industry 30 years ago as well as impossibility of the remaining domestic manufacturers to reoriente to the needs of rapidly developing market of components for laser technologies;

● difference in portion of distribution of laser material processing technologies (cutting, welding, heat treatment, engraving etc.) at Ukrainian enterprises from data of work [1].

Today, according to our data, application of laser cutting (estimated value around 65 % of total market of processing complexes) is dominant in the market of laser processing technologies in comparison with other technologies. Among the other laser processing technologies the most essential are laser marking (estimated value around 15 % of total market of processing complexes) and rapidly developing in the recent years technology of 3D-printing (estimated value around 10 % of total market of processing complexes). The market of technological complexes for processes of laser welding, heat treatment, piercing and other technologies, on our data, does not exceed 10 % of total market of the laser processing complexes. Change of the current situation with «shift» of demands of domestic market of the laser processing complexes to cutting and bringing it to the level of world standards, typical for market-economy countries, is possible by solving a series of the problems, one of which is development of domestic technologies and equipment for laser welding of different materials competitive in the world market.

Laser welding of metallic materials is used in development of structures for aircraft and marine ships, parts of medical equipment and assemblies of instrument-making as well as many other branches of industry. The scientific groups from E.O. Paton Electric Welding Institute, NTUU «Igor Sikorsky KPI» and other institutes of higher education as well as research laboratories of a range of large industrial enterprises successfully deal with the developments in the field of laser welding in Ukraine.

This work provides a review of a series of developments in the field of equipment and technology of

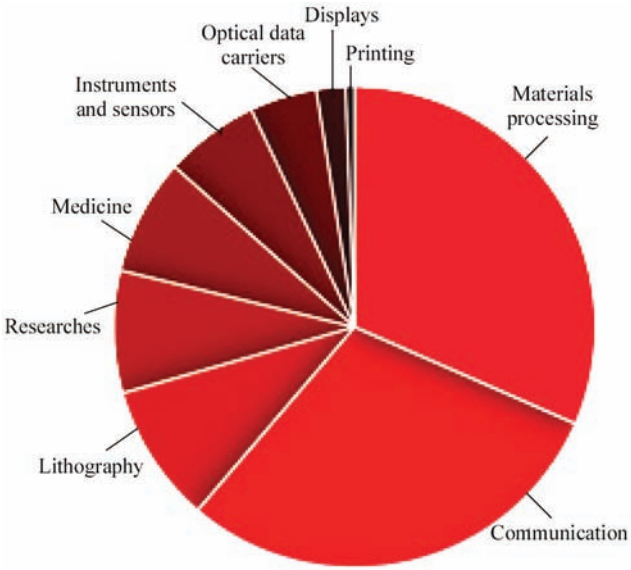

Figure 2. Distribution of application of laser units in the world for different branches of industry [2]

laser welding, which have been performed at the E.O. Paton Electric Welding Institute in the recent years, tested or implemented into industry.

E.O. Paton Electric Welding Institute in course of performance of scientific tasks has solved a problem on determination of the dependencies of effect of technological parameters of laser welding of thin-wall tubes on geometry and mechanical characteristics of received cold-rolled strip butt joints of δ = 0.15–0.2 mm thickness from high-alloy corrosion-resistant steels 12Kh18N10T (GOST 4986–79) and 1.4541 (DIN EN 10028-7:2000), taking into account the requirements of the next production of multilayer bellows from them [10]. It is determined based on the results of comparison of geometry, structure and mechanical properties of the produced joints that a determining parameter effecting the quality of this welded joint is a heat input, optimum range of variation of which lies in 3–5 J/mm limits. The results, obtained in course of work, made a basis for development of commercial technology of manufacture of straight thin-wall welded tubes of different diameter from stainless steels, applied for production of multilayer bellows on GOST 21744–83 (Figure 3). Such bellows are designed for operation as compensation elements, phase separators, sealing devices as well as elements of power assembly in the media promoting material corrosion at temperature from –260 to 550 °C.

Designed three-coordinate complexes of «ARMA-100M» type (Figure 4) for laser welding of straight thin-wall tubes of stainless steel are implemented at PJSC «KTsKBA» (Kiev) and «SRC»Armatom» LLC (Kiev). Application of developed technological recommendations and original technological fixture allowed providing productivity of one such complex up to 5 thou pcs of bellows billets per month. Finished products have been already used in different stop

Figure 3. Appearance of billet of multilayer bellows after hydroforming

valves operating in high-pressure pipelines at constant high-frequency and low-frequency vibration as well as stop assemblies requiring accurate positioning of a stop body. The multilayer bellows produced using laser welding are certified in accordance with the requirements of norms and rules as well as other reference documents in the field of nuclear power engineering.

The continuation of work mentioned above was development of a technology and fixture for laser welding of expansion bellows. They join parts and units, which in process of operation perform relative displacement or work under vibration conditions. The main operating element of these products is a bellows, that is flexible corrugated metallic tube of thin-wall stainless steel. The expansion bellows are produced by welding of a corrugated tube with a massive fixture (flanges, tubes, bushes etc.). Carried investigations showed that welding with pulse modulation of laser radiation is reasonable for manufacture of expansion bellows from stainless austenite steels. Techniques and equipment (Figure 5) were developed for laser welding of the expansion bellows. They allow getting fine grain structures, having increased mechanical characteristics level, in a cast weld metal and HAZ metal. This development was implemented at PJSC

Figure 4. Appearance of three-coordinate complex «ARMA-100M» for laser welding

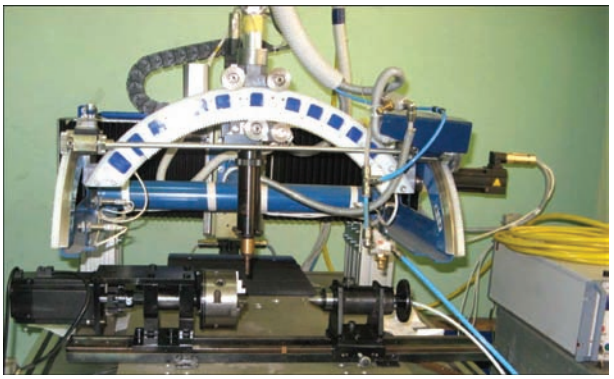

Figure 5. Technological complex for laser welding of expansion bellows

«Kiev plant «Analitpribor» and «SRC»Armatom» LLC for laser welding of probe housing (Figure 6).

S.M. Konyukhov Institute for strategic technologies (Dnepr) in a course of last years has been dealing with the problems of development of fundamentally new power unit of plasma engine PD140, which is used in a complex of cruise or adjustment-propulsion systems of rocket-space equipment. Manufacture of separate assembly elements of this power unit stipulates extremely rigid requirements on tailoring and quality of welding of its constituents. Together with PWI the works were carried out on approbation of laser tailoring technology and further laser welding without mechanical treatment of welded edges (250 pcs), parts of spiral heater of 0.25 mm thickness (produced from titanium alloy VT6). The results of work allow stating significant simplification of part edge mating and improvement of quality of welded joints. Researched level of mechanical characteristics indicates high reliability of the welded joints and perspective of application of these technologies in a rocket-space branch.

Different methods of arc fusion welding often apply a technique lying in filling of a gap between the edges being joined with molten filler metal [11]. The similar technique is rarely used for laser welding. There are usually concerns about minimizing a gap between the edges being welded and not using filler materials (to reduce energy consumption). We have proposed the method for joining the edges, which can not be tightly mated (for example, in the case of perforation). It is based on laser powder surfacing. The

Figure 6. Batch of expansion bellows manufactured using laser welding

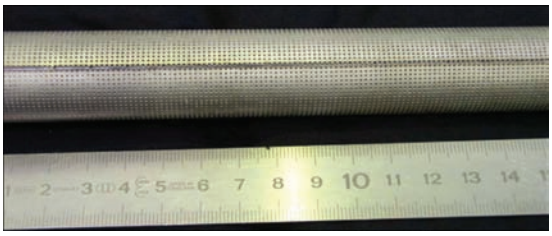

Figure 7. Housing of thin-wall tubular filter element manufactured on developed technology by laser welding with flux-cored wire

edges being welded are matched with small (up to one diameter of perforation hole) gap and tightly pressed to copper technological substrate. A proportioning feeder for supplying the filler powder of 60–100 μm granulation is used as auxiliary equipment. The filler material is selected depending on metal of edges being welded. In the process the gap is filled with powder, which is melted by laser radiation. Such an approach allows 10–30 % increase of coefficient of laser radiation absorption in comparison with simple welding. Laser welding of housings of tubular filter elements of δ = 0.5–0.6 mm wall thickness (steel Kh18N10T) (Figure 7) was carried out in accordance with the developed technology. Pilot batches of housings of the tubular filter elements, produced at PWI on the developed technology using laser welding with filler wire, were successfully tested and used in manufacture of elements for liquid filtering at «Chernovitskii chimzavod» ALC (Chernovtsy).

An instrument for manual laser welding of products (Figure 8), in particular, elements of internal structures of the cars for modern high-speed trains was developed to solve the tasks in the field of welding at carriage works (Changchun, PRC). Developed manual laser instrument is included in a content of the welding unit, which is manipulated by one operator-welder. Weight-dimension characteristics of the

Figure 8. Appearance of developed instrument for manual laser welding

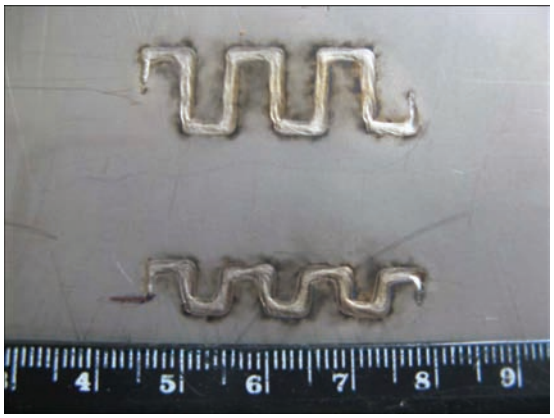

Figure 9. Appearance of welds produced on curved trajectory using instrument for manual laser welding

developed manual laser instrument allow carrying out welding in different spatial positions. Functional possibilities of the developed instrument permit to weld with movement of laser heat source at any set trajectory (Figure 9) within the limits of working field of 50×30 mm size. Carried metallographic examinations and mechanical tests of the lap welded joints of stainless steel 12Kh18N10T (plate thickness 2 mm), produced using developed manual laser instrument, showed that their mechanical characteristics are as good as the characteristics of the joints produced employing automatic laser welding.

Development and manufacture of the equipment (Figure 10) was carried out in order to perform research in the field of investigation of physics of the processes of combined impact on different metals of laser radiation with 1.07 μm wavelength and pulse arc plasma.

Figure 10. Appearance of developed working head for laser, microplasma and hybrid laser-microplasma welding

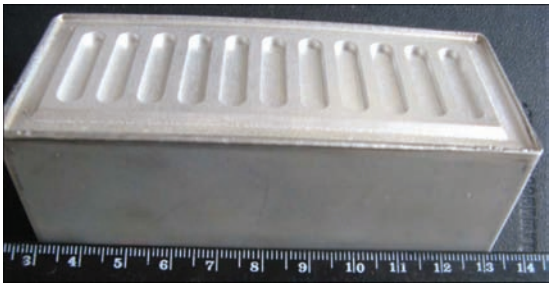

Figure 11. Appearance of fragment of accumulator housing of AMg6 (δ = 0.8 mm) alloy welded by closed weld using fiber laser radiation

The research was ordered by Harbin Welding Institute of China Academy of Machinery Science & Technology (Figure 10). A complex of devices was developed. It is designed for performance of the technological operations by laser, microplasma and hybrid laser-microplasma welding of thin-wall (0.1–2.0 mm) metals at direct, pulsed, alternating current with the possibility of separate regulation of amplitude and duration of current flow as well as effect of continuous or pulse laser radiation.

Other scientific developments of PWI in laser welding have passed industrial tests and approbation based on as series of Ukrainian and foreign aircraft- and rocket-building enterprises. Among them are welding of dissimilar materials (titanium alloys with aluminums); carbon with high-alloy stainless steels; welding with each other different grades of corrosion-resistant high-alloy steels etc.); welding of stringer panels and other elements of structures of aircrafts of titanium alloys [12]; butt welding of complex-profile reflective plates of nickel alloys; welding of casings of aluminum alloys (Figure 11); manufacture of different probes of high-alloy steels (Figure 12) and high-strength alloys.

Conclusions

1. Today the distinctive tendencies, typical for the Ukrainian market of material processing laser technologies, in comparison with the international market, are absence of domestic manufacturers of modern high-accuracy power laser units for material processing; loss of technology of manufacture of consumable components; prevailing demands on cutting equipment in the domestic market.

2. Increase of portion of laser welding in the domestic market is possible by means of development of domestic technologies and creation of the equipment for laser welding of different materials able to compete with leading world technologies.

3. Today laser welding technologies are essential for nuclear, chemical, instrument, aircraft and rocket construction branches of Ukrainian industry.

Figure 12. Housing of probe from steel 08Kh18N10T welded by laser radiation

4. High level of developments of E.O. Paton Electric Welding Institute in the field of technology and equipment for laser welding is verified by their relevance in the world's market.

1. Evstyunin, G.A. *Analysis of Russian and international market of laser technologies*. http://docplayer.ru/295602710Analiz-rossiyskogo-i-mezhdunarodnogo-rynka-lazernyh-tehnologiy-prezentaciya-k-kursu-lekciy-priglashyonnogo-specialista.html [in Russian].
2. *Annual laser market review & forecast: Can laser markets trump a global slowdown*? http://www.laserfocusworld.com/articles/print/volume-52/issue-01/features/annual-laser-market-review-forecast-can-laser-markets-trump-a-global-slowdown.html
3. *Lasers in the world and national market*. http://online.mephi.ru/courses/new_technologies/laser/data/lecture/1/p24.html [in Russian].
4. *Annual laser market review & forecast:Where have all the lasers gone*? http://www.laserfocusworld.com/articles/print/volume-53/issue-01/features/annual-laser-market-review-forecast-where-have-all-the-lasers-gone.html.
5. Tsukamoto, S. (2003) Laser welding. *Welding Int.*, 17(**10**), 767–774.
6. Yamaguchi, T., Katoh, M., Nishio, K. (2009) Mechanical properties of aluminium alloy welds by laser beam. *J. of Light Metal Weld. + Constr.*, **4**, 13–22.
7. Cao, X., Jahazi, M., Immarigeon, J.P., Wallace, W. (2006) A review of laser welding techniques for magnesium alloys. *J. Materials Proc. Technology*, 171(**2**), 188–204.
8. Schubert, E., Klassen, M., Zerner, I. et al. (2001) Light-weight structures produced by laser beam joining for future applications in automobile and aerospace industry. *Ibid*., 115(**1**), 2–8.
9. Chen, H.-C., Pinkerton, A.J., Lin Li (2011) Fibre laser welding of dissimilar alloys of Ti–6Al–4V and Inconel 718 for aerospace applications. *The Int. J. Adv., Manuf. Technol.*, 52(**9**), 977–987.
10. Shelyagin, V.D., Lukashenko, A.G, Lukashenko, D.A. et al. (2011) Laser welding of thin-sheet stainless steel. *The Paton Welding J.*, **4**, 38–42.
11. Shelyagin, V.D., Khaskin, V.Yu., Shitova, L.G. et al. (2005) Multi-pass welding of heavy steel sections using laser radiation. *Ibid.*, **10**, 46–49.
12. Paton, B.E., Shelyagin, V.D., Akhonin, S.V. et al. (2009) Laser welding of titanium alloys. *Ibid.*, **10**, 28–32.
13. Nikolov, M. (2014) Trends in development of weld overlaying during the 21st Century. *Acta Technologica Agriculturae*, 17(**2**), 35–38.

Received 07.11.2017

MACHINE VISION SYSTEMS
FOR PROCESSES AUTOMATION

Automatic joint tracking laser system for welding mills of pipe longitudinal welds ROVICOR STS-200-NS

The system is designed for automatic tracking of a joint center with groove preparation without filling or with partial filling after technological pass in arc welding or submerged arc welding.

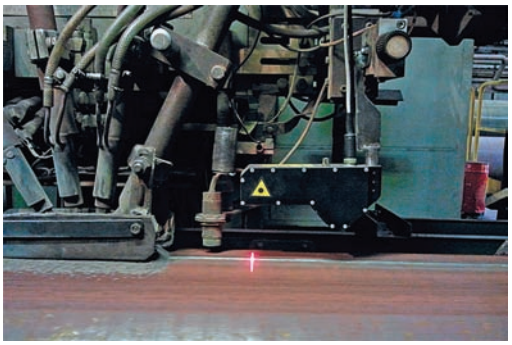

Laser weld tracking system for automatic ultrasonic testing of welded pipes ROVICOR SF-100

The system is designed for automatic tracking of a center of weld reinforcing bead during automatic ultrasonic testing of longitudinal pipe welds.

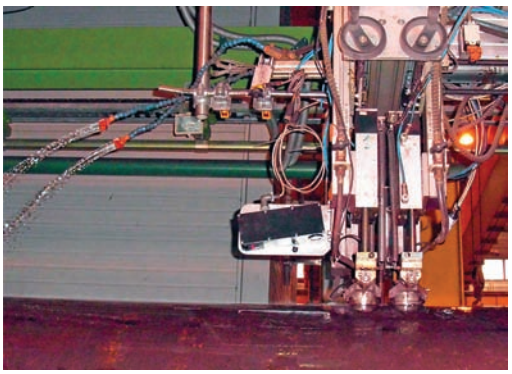

System for automatic detection of weld reinforcing bead and control of polymer dispenser in deposition of corrosion-resistant coating on welded pipe surface ROVICOR SFS – P08

The system is designed for detection of a center of weld reinforcing bead in pipe rotation and formation of signals for control of polymer dosage for providing uniform thickness of polymer coating on finished pipe (increase of dosage during polymer application on weld).

Laser joint tracking sensor for robotic arc welding ROVICOR STS-200-R

The laser sensor is designed for automatic balancing of the errors of workpiece assembly for welding by means of contact-free tracking of joint center in process of robotic arc welding.

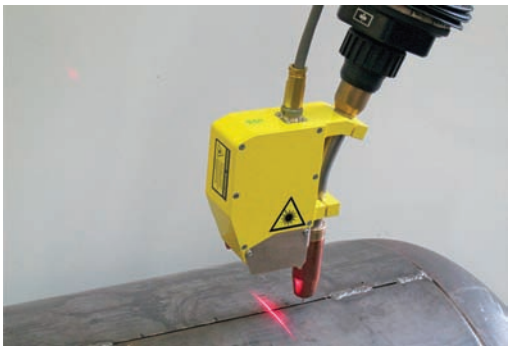

Developed by the E.O. Paton Electric Welding Institute of the NAS of Ukraine. E-mail: office@paton.kiev.ua

PATON PUBLISHING HOUSE

www.patonpublishinghouse.com

SUBSCRIPTION

«The Paton Welding Journal» is Published Monthly Since 2000 in English, ISSN 0957-798X, doi.org/10.15407/tpwj.

«Avtomaticheskaya Svarka» Journal (Automatic Welding) is Published Monthly Since 1948 in Russian, ISSN 005-111X, doi.org/10.15407/as.

«The Paton Welding Journal» is Cover-to-Cover Translation of «Avtomaticheskaya Svarka» Journal into English.

If You are interested in making subscription directly via Editorial Board, fill, please, the coupon and send application by Fax or E-mail.

The cost of annual subscription via Editorial Board is $348 for «The Paton Welding Journal» and $180 for «Avtomaticheskaya Svarka» Journal.

«The Paton Welding Journal» can be also subscribed worldwide from catalogues subscription agency EBSO.

SUBSCRIPTION COUPON

Address for journal delivery _____

Term of subscription since _____ **20** **till** **20** _____

Name, initials _____

Affiliation _____

Position _____

Tel., Fax, E-mail _____

We offer the subscription all issues of the Journals in pdf format, starting from 2009.

The archives for 2009–2016 are free of charge on *www.patonpublishinghouse.com* site.

ADVERTISEMENT

in «Avtomaticheskaya Svarka» and «The Paton Welding Journal»

External cover, fully-colored:
First page of cover (190×190 mm) — $700
Second page of cover (200×290 mm) — $550
Third page of cover (200×290 mm) — $500
Fourth page of cover (200×290 mm) — $600

Internal cover, fully-colored:
First/second/third/fourth page of cover (200×290 mm) — $400

Internal insert:
Fully-colored (200×290 mm) — $340
Fully-colored (double page A3) (400×290 mm) — $500

- Article in the form of advertising is 50 % of the cost of advertising area
- When the sum of advertising contracts exceeds $1001, a flexible system of discounts is envisaged

Size of journal after cutting is 200×290 mm

Editorial Board of Journals «Avtomaticheskaya Svarka» and «The Paton Welding Journal»
E.O. Paton Electric Welding Institute of the NAS of Ukraine
International Association «Welding»
11 Kazimir Malevich Str. (former Bozhenko Str.), 03150, Kiev, Ukraine
Tel.: (38044) 200 60 16, 200 82 77; Fax: (38044) 200 82 77, 200 81 45
E-mail: journal@paton.kiev.ua; www.patonpublishinghouse.com